

Cyclizations of Silyl Enol Ether Radical Cations – The Cause of the Stereoselectivity

Jens O. Bunte,^[a] Eike K. Heilmann,^[a] Birka Hein,^[a] and Jochen Mattay*^[a]

Keywords: Density functional calculation / Electron transfer / Radical cation / Silyl enol ether / Stereoselectivity

We have used photoinduced electron transfer (PET) activation of silyl enol ethers for the synthesis of tricyclic hydrocarbons. The mechanism of this reaction was investigated by conducting independent radical-induced cyclizations of corresponding iodo ketones and performing density functional theory (DFT) calculations on the possible intermediates. Our

aim was to explain the nature of the reactive intermediate of the cyclization step and to find the causes of the various types of selectivity observed in this process.

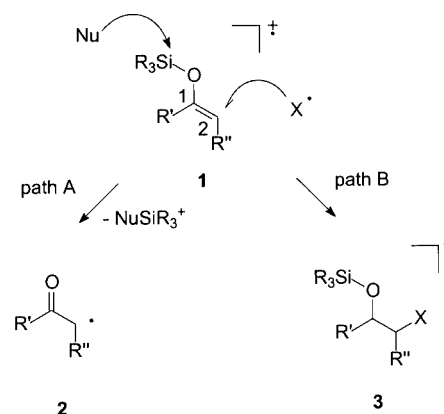
(© Wiley-VCH Verlag GmbH & Co. KGaA, 69451 Weinheim, Germany, 2004)

Introduction

Because of their electron-rich double bonds, silyl enol ethers have gained widespread use as nucleophiles in organic synthesis.^[1–3] In addition, the electron-rich character of these masked enol ethers or enolates can be used for oxidation reactions. A well-known example is the Rubottom oxidation with peracids or related oxygen-containing oxidants, which gives α -hydroxy ketones or silyl enol ether epoxides as products.^[4–13] One-electron oxidation can also be performed with silyl enol ethers: it results in the formation of radical cations.^[14] These highly reactive species can be generated by several means. Electrochemical oxidation has been applied for synthetic purposes^[15–17] and for mechanistic investigations.^[18] Reversible anodic oxidation during fast-scan cyclic voltammetric experiments provided strong evidence for the formation of radical cations.^[19] One-electron oxidation with chemical oxidants has been performed using cerium ammonium nitrate (CAN),^[19,20] tetranitromethane,^[21] and xenon difluoride,^[22] respectively. Furthermore, photoinduced electron transfer (PET) has been applied successfully;^[23–29] all transient species in the electron transfer process between chloranil and several silyl enol ethers have been investigated thoroughly by time resolved spectroscopy.^[24,25]

The primary product of the oxidation process, radical cation **1**, undergoes competing follow-up reactions (Scheme 1). The presence of nucleophiles (Nu) causes mesolytic cleavage of the Si–O bond, whereas bond formation

at the 2-position results from radical-type reactions, i.e., radical coupling or radical addition to double bonds.



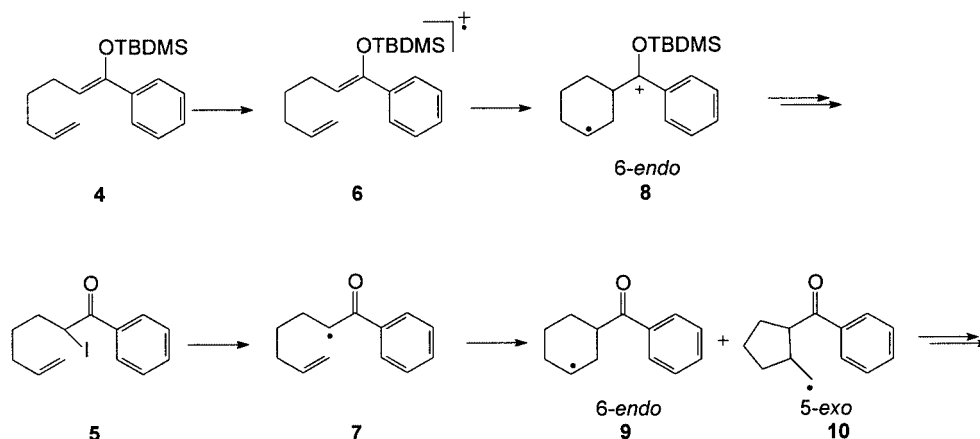
Scheme 1

The cleavage of the Si–O bond leads to the formation of α -carbonyl radicals **2** (path A), which also undergo radical reactions. The products of radical follow-up reactions of the primary radical cation **1** (path B), distonic radical cations or cations **3**, will also suffer loss of the silyl cation by nucleophilic substitution. An obvious and fundamental question is how these basic reaction steps are coupled in a reaction mechanism.

Snider et al. compared their results on the CAN-mediated oxidative cyclization of silyl enol ether **4** with Curran's results from atom transfer cyclization of **5**.^[20,30] They assigned the radical cation **6** to be the reactive intermediate for the cyclization reaction, because the cyclization mode was completely 6-endo selective (**8**), in contrast to the results from the atom transfer reaction, which proceeded via the α -carbonyl radical **7** (Scheme 2).

^[a] Organische Chemie I, Fakultät für Chemie, Universität Bielefeld, Postfach 100131, 33501 Bielefeld, Germany
 Fax: (internat.) +49-521-106-6417
 E-mail: mattay@uni-bielefeld.de

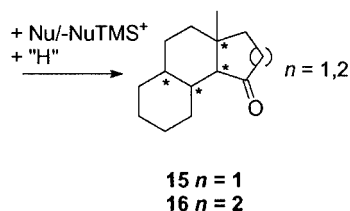
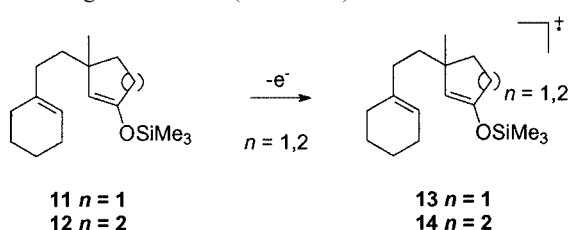
Supporting information for this article is available on the WWW under <http://www.eurjoc.org> or from the author.



Scheme 2

The influence of the reaction medium and, especially, its nucleophilic character is decisive for the mesolytic Si–O cleavage, as has been pointed out by Schmittel^[19] and Kochi.^[24,25] For example, addition of nucleophilic substances, such as alcohols, to a solution of silyl enol ethers in acetonitrile leads to an increase in the rate constant of Si–O cleavage. On the other hand, changing the solvent from polar, nucleophilic acetonitrile to less-polar, non-nucleophilic dichloromethane results in a slower Si–O cleavage and, additionally, in a different ion-pair dynamic, which leads to a different product spectrum.^[19,24,25]

In the course of our own research on the PET oxidations of silyl enol ethers, we have found high selectivities occur during the formation of polycyclic hydrocarbons, like **15** and **16**, from silyl enol ethers. In addition to complete 6-endo selectivity in the cyclization step, high stereoselectivity has also been observed to occur in the formation of three new stereogenic centers (Scheme 3).^[31]



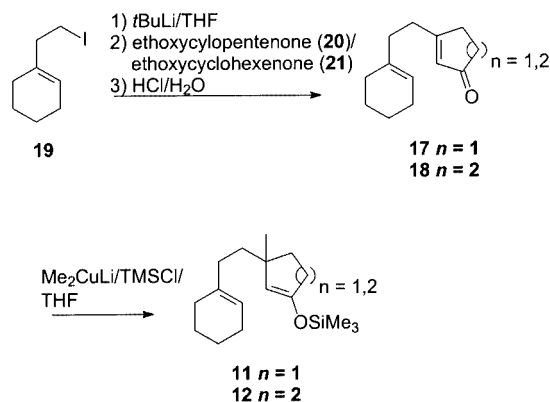
Scheme 3

In this paper, we present the results of our studies regarding the nature of the reactive intermediates involved as well as the causes of the selectivities observed.

Results and Discussion

PET Oxidative and Radical Cyclizations

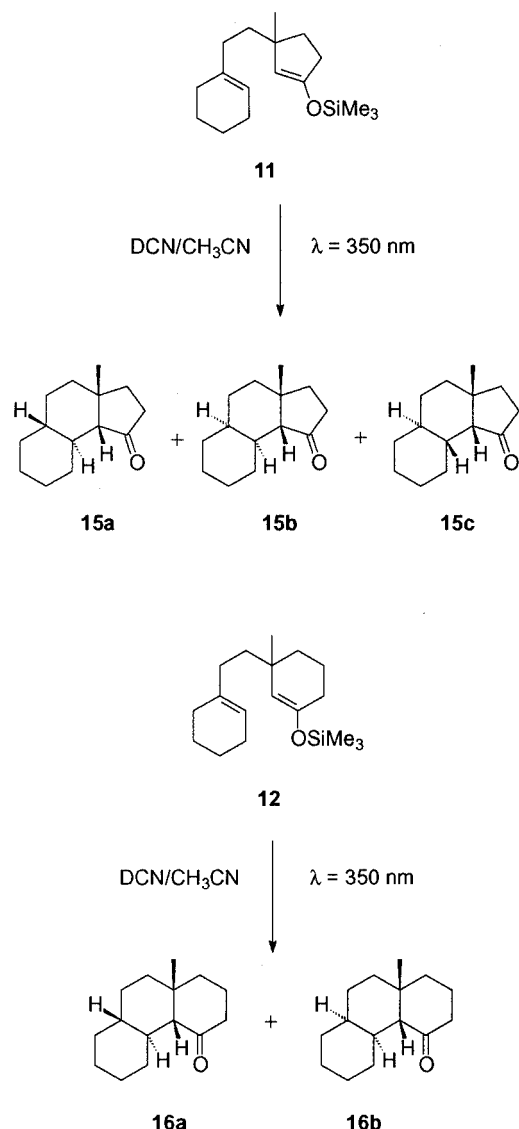
As reported earlier, we have synthesized the silyl enol ethers **11** and **12** from the corresponding cycloalkenones **17** and **18** by reaction with dimethyl cuprate and trimethylsilyl chloride (Scheme 4) and subjected them to PET oxidative cyclization with 1,4-dicyanonaphthalene (DCN).^[32]



Scheme 4

Cyclization of **11** resulted in the formation of three diastereoisomers, **15a**, **15b**, and **15c**, respectively; their product ratio was 41:31:28 (Scheme 5; as throughout the text, only one enantiomer is shown for the sake of clarity). Obviously, only 6-endo-cyclized products were formed from the primary radical cation of **11**. Additionally, we observed a complete *cis*-selectivity with respect to the methyl group and the α -carbonyl hydrogen atom. Interestingly, the relative stereochemistry at the remaining two stereogenic centers varies with low selectivity, in contrast to the cyclization of **12**, in which only two diastereoisomers were observed with a 90:10 selectivity.

Focusing on silyl enol ethers derived from cycloalkenones bearing a cyclohexenyl side chain, we were able to investigate three different aspects of the selectivity in the cycliza-



Scheme 5

tion reaction. As mentioned before, the ring-size selectivity in the formation of distonic radical cations **22** and **23** was found to be 6-*endo*. This feature of the PET oxidative cyclization of silyl enol ethers was observed earlier, where it was attributed to the radical cations being the reactive intermediates in the cyclization step (Scheme 6).^[27,29] Additionally, the relative stereochemistry of three of the four stereogenic centers is determined in the cyclization step (**22**, **23**). The third selectivity in the transformation is the saturation reaction of the remaining radical center. This formal hydrogen atom addition generates the fourth stereogenic center. The nature of this process is not fully understood yet. Recent studies from our group, utilizing deuteration experiments, indicate that tertiary radical centers, like **22** and **23**, are saturated via an electron transfer/protonation sequence.^[32] The source of the electron is the radical anion of

the sensitizer, whereas the proton is transferred from residual water and the solvent (acetonitrile).

With the differences in selectivity of the cyclization of silyl enol ethers **11** and **12** measured, we were faced with the questions of how the ring size of the silyl enol ether influences the product distribution and, in a broader context, how the reaction proceeds mechanistically.

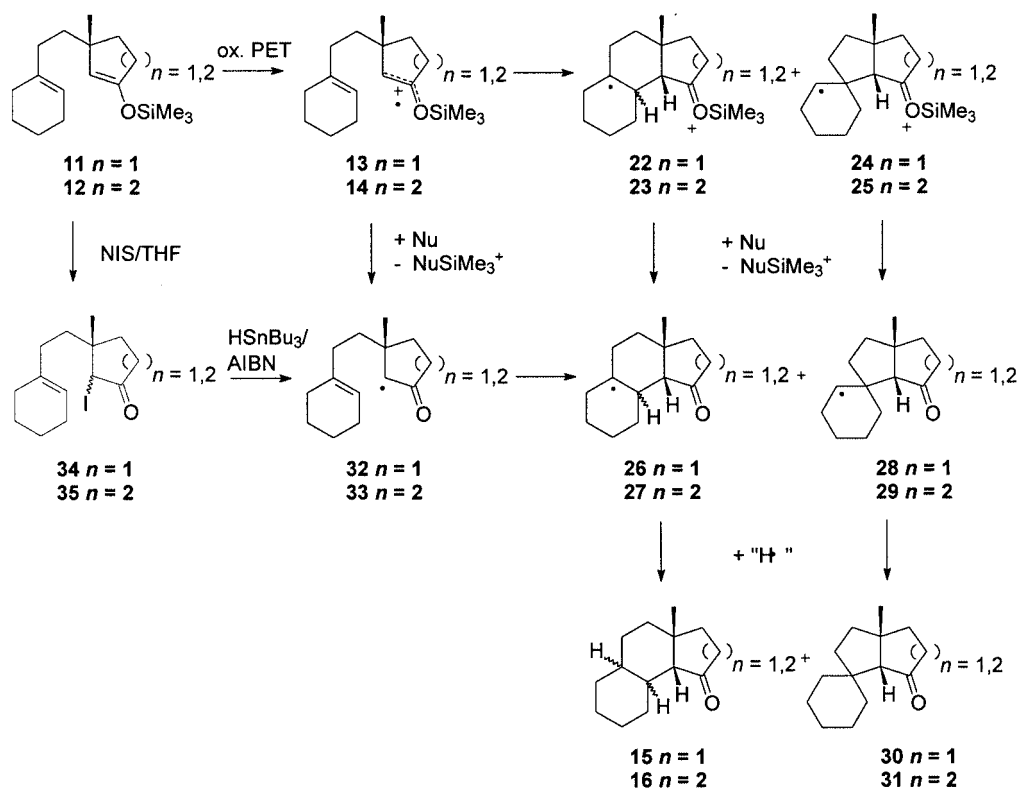
The complete transformation (**11** → **15** or **12** → **16**) comprises four different steps: one-electron oxidation, ring closure, mesolytic Si–O cleavage, and saturation of the radical position. The one-electron oxidation can be identified as the initiating step and the radical saturation as the terminating step, but the sequence of ring closure and Si–O cleavage has not yet been determined (Scheme 6).

Generally speaking, the sequence of cyclization and Si–O cleavage determines the intermediate in the cyclization step and it is, therefore, essential for the understanding of the processes involved in product formation. Because 6-*endo* selectivity within the cyclization step was considered to be the result of radical cations being the reactive intermediates, we tried to prove this hypothesis by the selective generation of α -carbonyl radicals **32** and **33** and investigating the product distribution. α -Carbonyl radicals were generated by iodine abstraction from α -iodo ketones utilizing the tin hydride method.^[33,34] Consequently, iodo ketones **34** and **35** were prepared from silyl enol ethers **11** and **12** by reaction with *N*-iodosuccinimide (NIS);^[35,36] **34** and **35** were obtained in 77 and 83% yields, respectively, as light-, air-, and temperature-sensitive oils (Scheme 6).

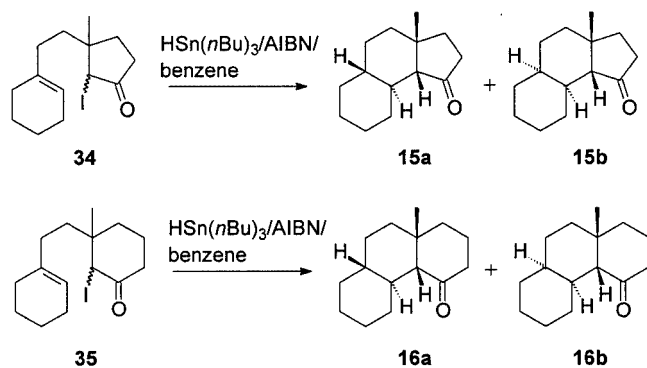
Both iodo ketones are 1:1 mixtures of diastereoisomers; they differ with respect to the positioning of their methyl group and iodine substituent. The structures were assigned using ¹H and ¹³C NMR spectroscopy and mass spectrometry. Because of their instability, mass spectra of the iodo ketones could only be obtained by ESI/MS using their hydrazone derivatives.

The reaction of **34** with tributyltin hydride afforded a mixture of **15a** and **15b** in 42% yield after chromatographic purification (Scheme 7). The diastereoisomeric ratio was 58:42, as determined by GC analysis of the crude reaction mixture. Compound **35** was cyclized by the same means, affording **16a** and **16b** as a 90:10 mixture of diastereoisomers in 33% yield.

Comparison with the results from the PET oxidative cyclization of these cyclohexane-derived species (Scheme 5) revealed several interesting aspects. Most remarkably, the same products were formed by the radical (from **35**) and PET oxidative cyclization (from **12**). Furthermore, the product ratios are identical. The follow-up reactions of α -carbonyl radical **33** resulted only in the formation of 6-*endo*-cyclized products. The complete lack of 5-*exo* products was unexpected from this radical-type species. The stereoselectivity in the cyclization step was also fully *cis-transoid* (radical **27**) as it was in the PET reaction. The saturation process of radical **27** resulted in the same high diastereoselectivity as that observed for the PET process, although the hydrogen source was completely different. Tributyltin hydride is significantly more bulky than the ex-



Scheme 6



Scheme 7

pected sources of hydrogen or protons in the PET case, and the saturation occurs through a radical pathway.

The cyclization of cyclopentanone-based iodo ketone **34** led to the formation of only two diastereoisomers, **15a** and **15b**. In contrast to the PET-mediated cyclization, the *cis-cisoid* product **15c** was not formed in the radical cyclization reaction. The ratio of **15a** to **15b** (1.38) was similar to the ratio of **15a** to **15b** obtained in the PET reaction (1.32), which displays a low selectivity in the saturation step. The missing third isomer gave a first hint that different reactive intermediates exist in both cyclization procedures (radical vs. PET).

The Radical Reaction Pathway

Further insight into the details of the radical cyclization of iodo ketones **34** and **35** was obtained through calculations on the reaction profile.^[37] Energy calculations of the radical intermediates of the cyclization reaction, as well as transition state geometry calculations, were performed on the density functional theory (DFT) level, which is known to produce good results for this task.^[38,39] From the variety of potential combinations of calculation methods and basis sets, we found that a combination of the B3LYP functional^[40,41] and the 6-31G* basis set^[42] gave good results for these complex structures with an acceptable demand in CPU time.^[43]

Calculations on the cyclopentanone system **32** started with energy calculations on the four possible cyclized radicals (**26a**, **26b**, **28a**, and **28b**) as well the initial radical **32**. Additionally, we calculated the transition state geometries leading to the cyclization products (Figure 1).

All energy values are displayed in kcal/mol and are referenced to the starting radical **32**. In addition, the energy values for the transition states are compared to the lowest-energy transition state leading to **26a**. To ensure that the calculated energies are indeed the lowest possible energies for these highly flexible intermediates, we applied a multistep calculation strategy. Starting with the cyclized radicals **26a**, **26b**, **28a**, and **28b**, we performed conformational analyses on a semiempirical level (AM1). For each of the obtained conformers, we calculated a reaction path con-

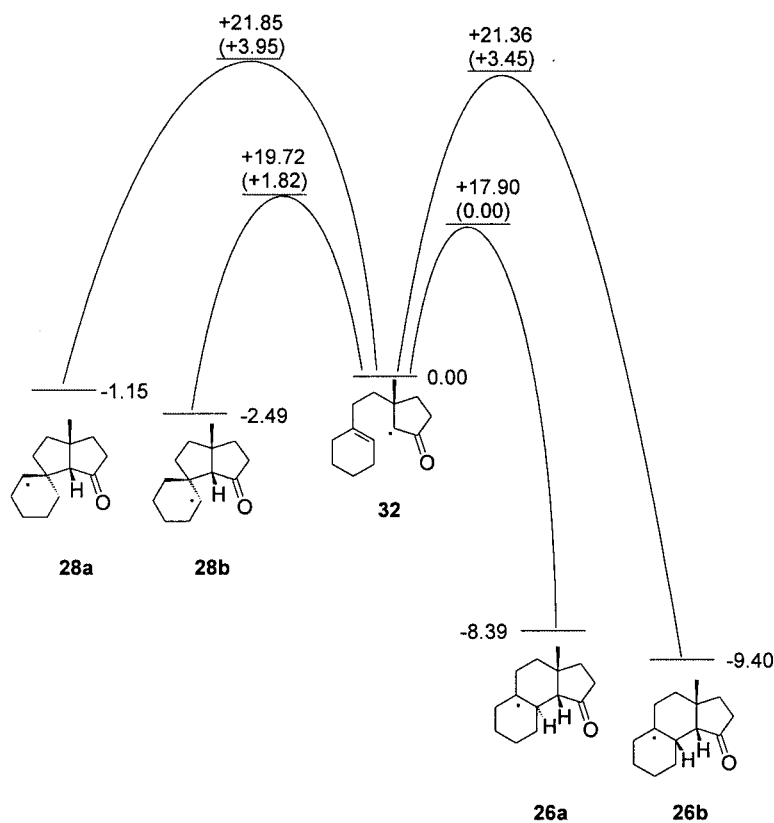


Figure 1. Calculated energy profile for radical **32**

cerning the bond of interest. From these profiles, the transition states were calculated on a semiempirical level (AM1). Finally, from this collection, we calculated the lowest transition states at the B3LYP/6-31G* level, applying frequency analysis to ensure that the intermediate is a transition state. Energy calculations of the cyclized radicals were conducted in the same way. For energy comparison, we applied zero point energy correction. The analogous energy profile for the cyclohexanone system **33** is shown in Figure 2.

As we observe from Figures 1 and 2, cyclization of starting radicals **32** and **33** cannot be described easily by means of kinetic control. The 6-*endo* cyclization pathways are considerably exothermic, whereas the 5-*exo* cyclization leads to radical intermediates that are either slightly exothermic (**28a**, **28b**) or endothermic (**29a**, **29b**) when compared to the starting radicals. The reason for these thermodynamics lies in the highly stabilized character of the α -carbonyl radicals **32** and **33**.

The geometries of the transition states leading to the cyclized radical intermediates shown in Figures 1 and 2 can be described using the Beckwith–Houk model for the cyclization of hexenyl radicals.^[44–46] The lengths of the bonds formed are 2.14 Å for the 6-*endo* cyclizations and 2.19 Å for the 5-*exo* cyclizations, which are in the typical range for comparable radical cyclizations.^[34] The transition states for the cyclizations to **27a** and **27b** are shown in Figure 3.^[47]

The central six-membered rings of the 6-*endo* transition states can be described as stretched cyclohexane conformers. We observe in Figure 3 that the transition state leading to *cis-transoid* radical **27a** shows a chair-like conformer, whereas **27b** should be formed via a twist-like conformer in the corresponding transition state. This finding is in good agreement with the energy difference of 3.45 kcal/mol between these two structures. In another view, both carbocyclic rings of the starting radical **33** approach in a coplanar manner to reach the low-energy transition state leading to **27a**, whereas they must approach in a stack-like arrangement for the formation of the *cis-cisoid* radical **27b**.

One of the questions we had to face was the origin of the *cis-cisoid* cyclization product **15c** in the PET oxidative cyclization (Scheme 5); this compound is not formed in the radical reaction and, furthermore, it occurred only in the cyclopentanone system. In agreement with the calculated energy values, we did not observe this stereochemistry in the radical cyclization of iodo ketone **34**. At a reaction temperature of 80 °C in refluxing benzene, an energy difference of 3.45 (**26a**, **26b**) or 3.72 kcal/mol (**27a**, **27b**) between the transition states would lead to an amount of <1% of the product from the high-energy transition state. Thus, the reason for stereoselective 6-*endo* ring closure in the radical cyclization path can be seen in the clearly disfavored twist-like transition state for the *cis-cisoid* approach in **26b** and **27b**.

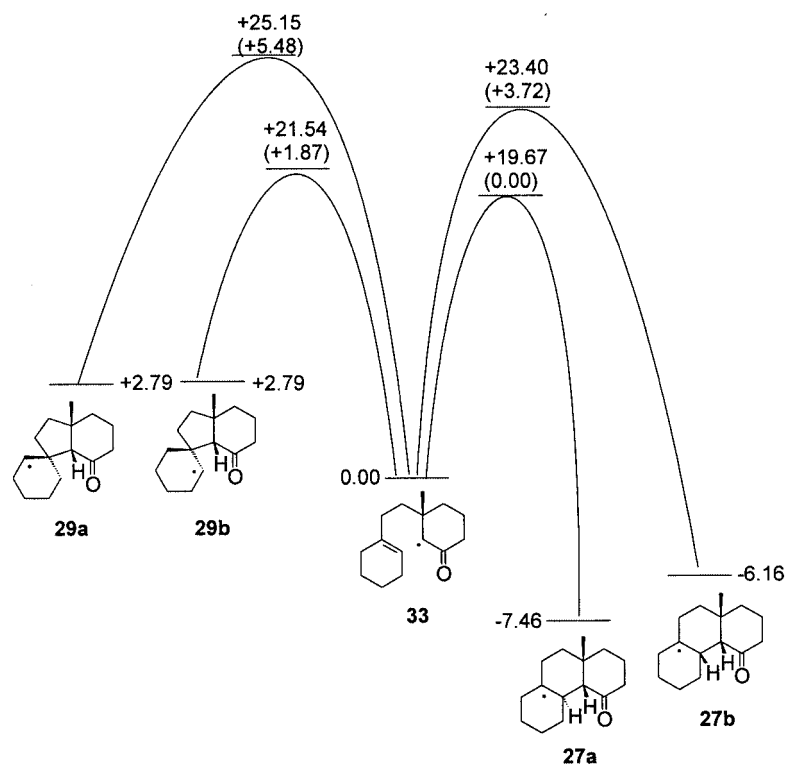


Figure 2. Calculated energy profile for radical **33**

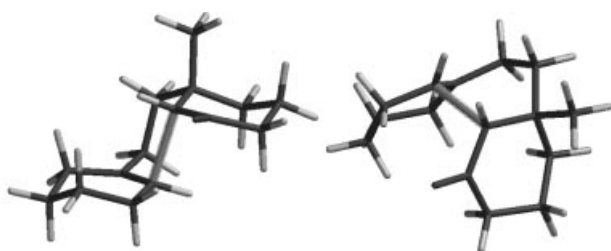
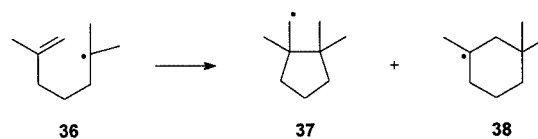


Figure 3. Transition states of the formation of **27a** and **27b**

Considering the same kinetic-control approach for the low-energy transition states for the 5-*exo* cyclization (**28b**: 1.82 kcal/mol; **29b**: 1.87 kcal/mol), 7% of the product should have been isolated. The lack of these products can be explained by assuming a reversible 5-*exo* cyclization, which is feasible when considering the energetic situation. Besides suitable thermodynamics, a necessary requirement for a reversible ring closure is a lifetime of the intermediates that allows both cyclization and ring opening prior to a follow-up reaction. In this case, the follow-up reaction is the hydrogen transfer from tributyltin hydride. For secondary radicals, a rate constant of $1.5 \times 10^6 \text{ L mol}^{-1} \text{ s}^{-1}$ has been determined at 298 K; for tertiary radicals, the rate constant is $1.7 \times 10^6 \text{ L mol}^{-1} \text{ s}^{-1}$ at 303 K.^[48] As is noticeable from these values, no sufficient differentiation between secondary and tertiary radicals in the saturation reaction can be achieved.

A reasonable value for the rate constant of the cyclization reaction of radicals **32** and **33** can be estimated from the

related cyclization of hexenyl radical **36**. The rate constant for the 5-*exo* cyclization was determined to be $2.6 \times 10^6 \text{ s}^{-1}$, whereas the 6-*endo* cyclization proceeds with a rate constant of $2.0 \times 10^6 \text{ s}^{-1}$ at 313 K (Scheme 8).^[49]



Scheme 8

Assuming the radical concentration is equal for both the cyclization and saturation reaction and setting the concentration of tin hydride to the concentration of 50% conversion ($2.5 \text{ mmol} \cdot \text{L}^{-1}$), we obtained values of $v_{\text{cyc}}/[\text{rad}] = 2 \times 10^6 \text{ s}^{-1}$ for the cyclization and $v_{\text{sat}}/[\text{rad}] = 4 \times 10^3 \text{ s}^{-1}$ for the saturation reaction.

Using this simplified expression with one constant concentration for all radical species and neglecting temperature dependencies of the values known in the literature, we find a cyclization rate 500 times faster than the saturation process. Further evidence for the slow saturation is the lack of uncyclized material. α -Carbonyl radicals **32** and **33** did not react with tributyltin hydride, but underwent complete cyclization. The assumed ratio between the cyclization and saturation kinetics results in a reversible 5-*exo* cyclization and, consequently, the observed 6-*endo* selectivity of the radical cyclization of iodo ketones **34** and **35**.

In the case of tributyltin hydride, the stereoselectivity of the saturation of the intermediately formed radicals **26a** and **27a** is determined by the energy differences of the transition states. The calculation of these large, highly flexible structures, or of simplified trimethyltin hydride species, could not be accomplished sufficiently on the DFT level. The strong exothermic character of the saturation reaction allows Hammond's postulate to be used and, therefore, it should be possible to describe the observed selectivity in the saturation process using the conformer energies of the cyclized radicals. For the cyclohexanone species **27a**, two conformers are of major interest (Figure 4). Conformer **27a1**, formed directly via the transition state shown in Figure 3, can react with tributyltin hydride to form product **16b** through *cis*-saturation. Because of the slow reaction with tributyltin hydride, **27a1** can equilibrate with **27a2**, which is 2.02 kcal/mol more stable. Reaction of **27a2** with tributyltin hydride leads to the formation of the *trans*-saturated product **16a**. According to Hammond's postulate, this energy difference results in the diastereoselectivity of the saturation process. At a reaction temperature of 353 K, the energy difference of 2.02 kcal/mol leads to 6% of the *cis*-saturated isomer **16b**. Indeed, this yield is close to the observed value of 10% for **16b** in the reaction product of the radical cyclization of **35**.

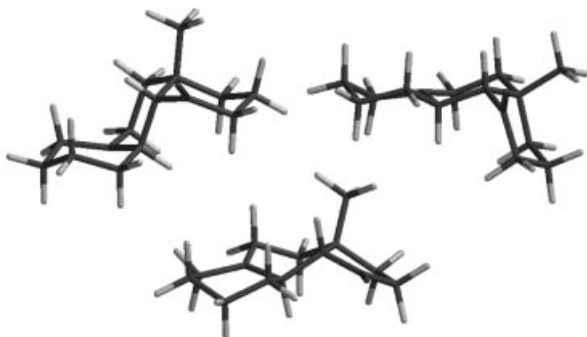


Figure 4. Structures of **27a1**, **27a2**, and **26a**

Unlike **27a**, cyclopentanone radical **26a** does not have a preferred conformer. As a consequence of the less-flexible cyclopentanone ring bearing substituents with dihedral angles of nearly 0°, the central six-membered ring is forced into twist- or boat-like conformations. In these very similar conformers, the lowest-energy form of which is shown in Figure 4, the radical position is flattened. This observation contrasts with the geometric features of the conformations of **27a**, where the radical center is pyramidalized towards the site where the reaction with tin hydride occurs. The geometrical features of the conformers of **26a**, in combination with the similar energies for the conformers, explain the observed lack of selectivity in the saturation process.

In summary, we were able to explain sufficiently all the selectivities observed in the cyclization process. (a) The 6-*endo* selectivity can be realized by a reversible 5-*exo* cyclization that becomes possible as a result of the stabilized α -carbonyl radicals. (b) The reversibility can be explained

by a comparison of the rate constants of the involved processes and is further supported by the fact that only cyclized products were isolated. (c) The exclusive *cis-transoid* stereochemistry found in the cyclization products can be rationalized by kinetic control; the competing *cis-cisoid* stereochemistry could be formed only via a high-energy transition state. (d) Finally, the stereoselectivity of the saturation process can be explained well using Hammond's postulate and comparing the energies of the conformers of the radicals involved. Differences in the observed selectivities between cyclopentanone and cyclohexanone systems were observed only in the last step, the radical saturation. Because of the rigid cyclopentanone ring, the cyclized radical could not reach the stable conformation that formed in the cyclohexanone system.

It should be noted that we were able to demonstrate that an observed 6-*endo* selectivity cannot be attributed simply to a radical cationic reaction intermediate, as it has been described previously.^[29] The results of the radical cyclizations demonstrate that the question concerning the reaction mechanism of the PET oxidative cyclization has yet to be answered.

The Radical-Cationic Reaction Pathway

Prior to investigating the cyclization reactions of silyl enol ether radical cations, we tried to characterize the reactive site of the radical cation generated by one-electron oxidation by utilizing DFT calculations. We were interested in the distributions of charge and spin, where a comparison with the corresponding α -carbonyl radical was possible. As a model system for calculation, we chose 3,3-dimethylcyclopentanone. Comparison of the calculated structures (using B3LYP/6-31G*) of silyl enol ether **39** and its corresponding radical cation **40** revealed several changes in the molecular structure induced through oxidation (Figure 5).

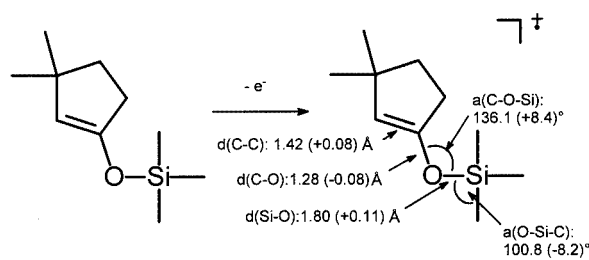


Figure 5. Geometrical changes of **39** induced by one-electron oxidation

As expected, one-electron oxidation weakens the C–C double bond because this position is the most electron-rich. This process is accompanied by a strengthened C–O bond, as can be estimated by their bond lengths. The second important structural change concerns the silyl moiety. The O–Si bond is weakened and the three methyl groups possess a more-planar orientation. The length of the O–Si bond (1.80 Å) can be compared directly with structures calculated by Olah for adducts between the trimethylsilyl cation and several carbonyl compounds; for these systems,

lengths of 1.8 Å for O–Si bonds were also found.^[50] Additionally, the X-ray structure of the cation formed from the triisopropylsilyl cation and acetonitrile can be used for comparison.^[51,52] Here, a value of 1.82 Å has been reported for the length of the O–Si bond.

All the geometrical features found in these calculations are in agreement with the expected properties of the radical cations: the weakened O–Si bond leads to an easy S_N2-like substitution of the silyl cation induced by the solvent or other nucleophiles. The bond orders of 1.5 for both the C–C and C–O bonds can be attributed to a heteroallylic system corresponding to an α -carbonyl radical. To determine the influence of the attached trimethylsilyl cation on the spin distribution, we calculated the distribution for the α -carbonyl radical **41** for the sake of comparison (Figure 6).

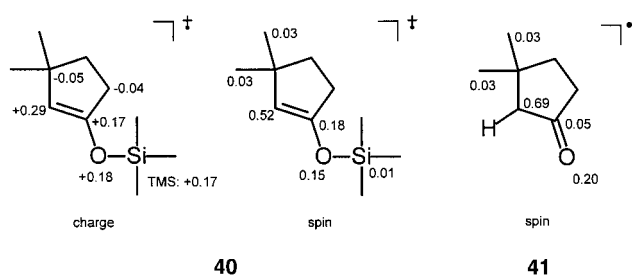


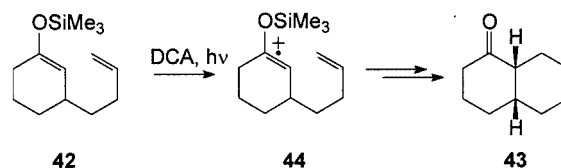
Figure 6. Calculated distributions in **40** and **41**

As expected for this heteroallylic system, the spin density is located at both ends of the three-atom arrangement. About 70% of the spin density is located at the α -position, which is the reactive position for follow-up reactions.

In contrast, the corresponding radical cation **40** shows a delocalized spin distribution. Only 52% of the spin is localized at the reactive α -position. The carbonyl group contributes further, showing a strong disturbance of the former heteroallylic system. The silyl group does not carry any spin.

To achieve a comparison between partial charges in the neutral silyl enol ether **39** and its radical cation **40**, we calculated natural bond orbital (NBO) charges for both.^[53–56] The observed differences are shown in Figure 6. The trimethylsilyl group contributes to only 17% to the positive charge; this finding contrasts the view that it is a cationic leaving group. Obviously, the ease of Si–O cleavage must be explained by the substitution reaction mentioned above. The remaining charge is delocalized over the carbonyl group and its α -position. This cationic character of the reactive site must be considered for the estimation of the reactivity of the radical cation.

The effect of the electrophilic reactive site can be seen clearly from calculations we conducted for one of our earlier cyclization reactions.^[29] As demonstrated experimentally, butenyl-substituted cyclohexanone silyl enol ether **42** cyclizes in a complete 6-*endo* fashion under PET oxidative condition to yield *cis*- α -decalone **43** (Scheme 9).



Scheme 9

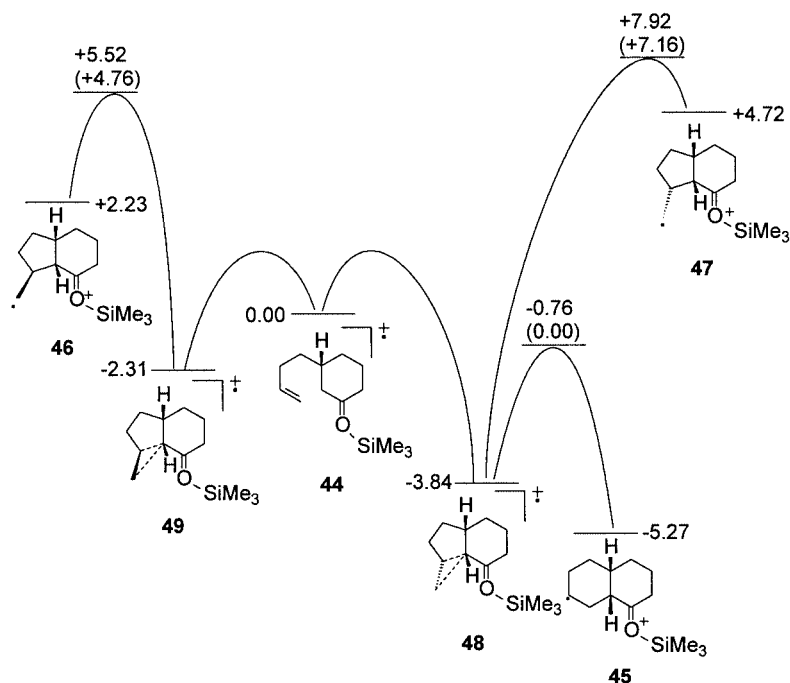
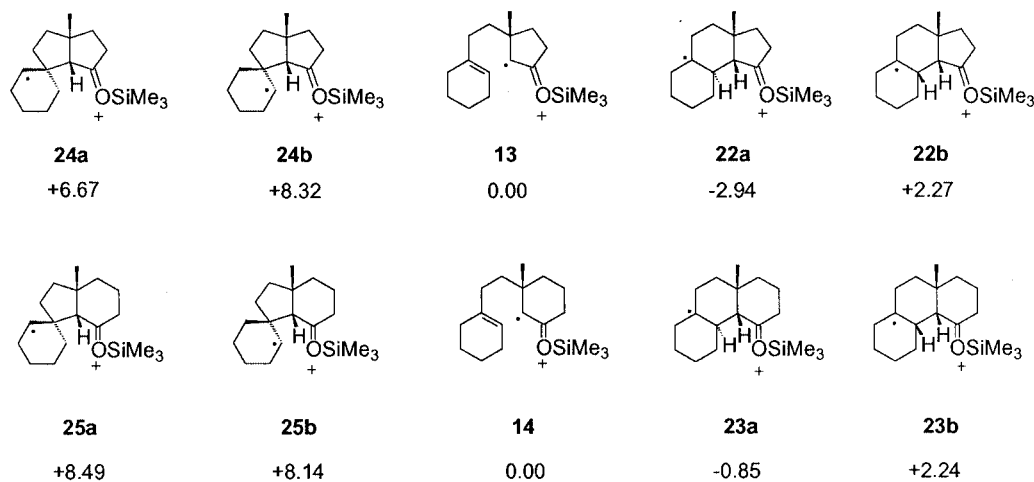
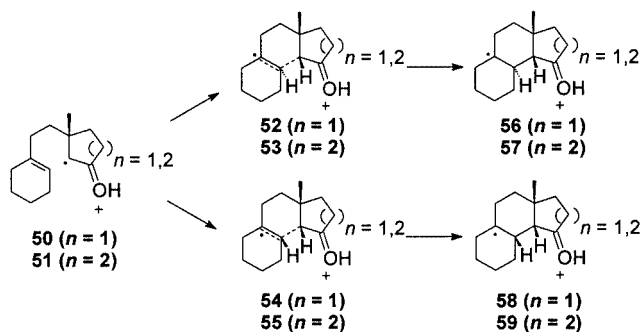
We calculated the energy profile for the possible cyclization products of radical cation **44** and the corresponding transition states by the methodology described above. As seen from Figure 7, the transition states for the 5-*exo* products **45** and **47** are too high in energy to contribute to the product distribution. The 5-*exo* cyclization also proceeds endothermally. As a direct consequence of the cationic character of the intermediates, additional minima were found on the energy surface.

Structures **48** and **49** can be described as electron-deficient compounds carrying a bond between the radical cationic center and the double bond.^[48] The bond length was calculated to be 2.8 Å and, thus, clearly it is less than double the van der Waals distance of a typical *p*-system. The α -carbonyl position is located in a 5-*exo* orientation towards the double bond. Because of the weak character of this bond, it can slip easily along the π -system to achieve a 6-*endo* cyclization. This process can be seen clearly from the energy of the transition state leading to **45** (Figure 7). Thus, the observed 6-*endo* selectivity of the PET oxidative cyclization reaction of **42** can be explained reasonably by the energy profile calculated on the DFT level.

We continued with calculations of the energy profiles of radical cations **13** and **14**. Unfortunately, it was not possible to calculate the transition state geometries for these cyclizations because the highly flexible character of the intermediates prohibited successful geometry optimizations for the transition states. The energies of the stationary points are displayed in Scheme 10.

Even without the accurate energy values for the transition states, it becomes obvious from Scheme 10 that the 5-*exo* cyclization is disfavored. The formation of 5-*exo*-cyclized products is endothermic [6.7 (**24a**) and 8.5 (**25a**) kcal/mol] and will, therefore, not contribute to product formation. To explain the stereoselectivity in the cyclization reaction, we chose to calculate simplified radical cations to learn more about the transition state energies. The replacement of the trimethylsilyl cation by a proton gave the radical cations shown in Scheme 11.

We calculated the transition state geometries **52–55** and found an energy difference of 1.77 kcal/mol between **52** and **54**.^[48] This value is clearly less than that (3.45 kcal/mol) in the corresponding radical cyclization (Figure 1) and, thus, it provides a first hint towards the cause of the observed product distribution. In contrast, the corresponding *cis-cisoid* transition state **55** could not be calculated. Since we could not identify a transition state for the reaction **51** \rightarrow **59**, we calculated reaction profiles for both **51** \rightarrow **59** and

Figure 7. Calculated energy profile for radical-cation **44**Scheme 10. Energetics of possible cyclization products of **13** and **14** (in kcal/mol)

Scheme 11

the corresponding cyclohexanone system **50** → **58**. The results of these DFT calculations are shown in Figure 8.^[57] The bond of interest was opened in steps of 0.10 Å. Cyclohexanone radical cation **59** does not represent a minimum on the energy surface, which is in sharp contrast to the cyclopentanone radical cation **58** (Figure 8). Although this result explains why transition state **55** could not be calculated, it should be considered that these calculations were conducted using a simplified system. The corresponding trimethylsilyl radical cation **23b** (Scheme 10) is indeed a minimum, although no follow-up products could be isolated.

According to the results in Figure 8, the reason for the differences in the product distribution between cyclopentanone and cyclohexanone silyl enol ether radical cations **13**

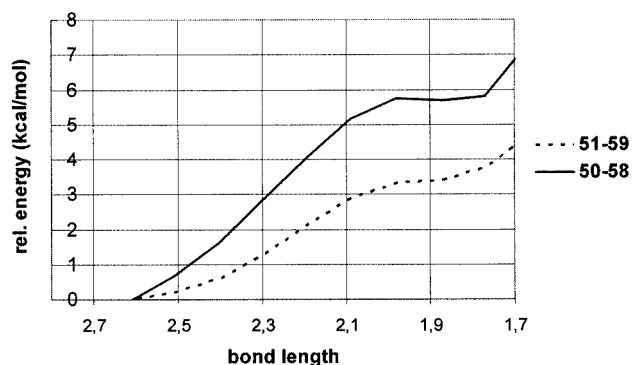
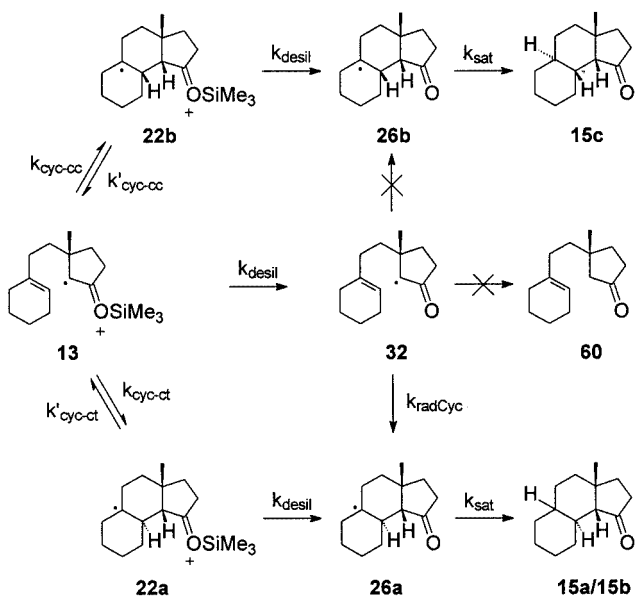


Figure 8. Calculated energy profiles for the cyclizations **50** → **58** and **51** → **59**

and **14** could be a result of the different lifetimes of the corresponding *cis-cisoid* cyclized radical cations **22b** and **23b** (Scheme 12). Both cyclizations from starting radical cations **13** and **14** are endothermic, but only in case of **22b** was follow-up product **15c** isolated.

As for the radical cyclization process described earlier, the kinetics of the follow-up reactions must be considered to describe the reaction mechanism properly. These reactions are the mesolytic cleavage of the Si–O bond and the saturation of the remaining radical position. The possible reaction pathways for radical cation **50** are displayed in Scheme 12.

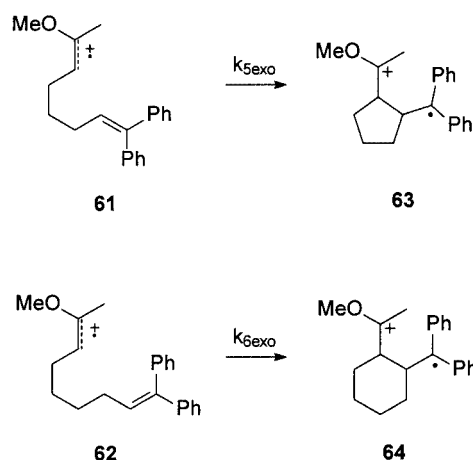


Scheme 12

Starting from **13**, two 6-*endo* cyclization reactions are possible, leading to either **22a** or **22b**. Additionally, desilylation to **32** can occur, which cannot explain the formation of **15c**, as shown for the radical cyclization of iodo ketones. Because of the energetics of both cyclization reactions (**22a**, **22b**), reversibility must be taken into account. The final saturation process seems to have no influence on the selec-

tivity of ring closure, because no uncyclized ketone **60** could be detected.

Reactions of radical cations are generally considered as very fast processes as a result of the flattened energy surface.^[58] It is rare to find values for the rate constants of cyclization reactions that are similar to those of our system. Recently, Horner et al. investigated the cyclization of enol ether radical cations and determined the rate constants for these processes.^[59] Examples for a 5-*exo* and a 6-*exo* cyclization of radical cations **61** and **62** are shown in Scheme 13.



Scheme 13

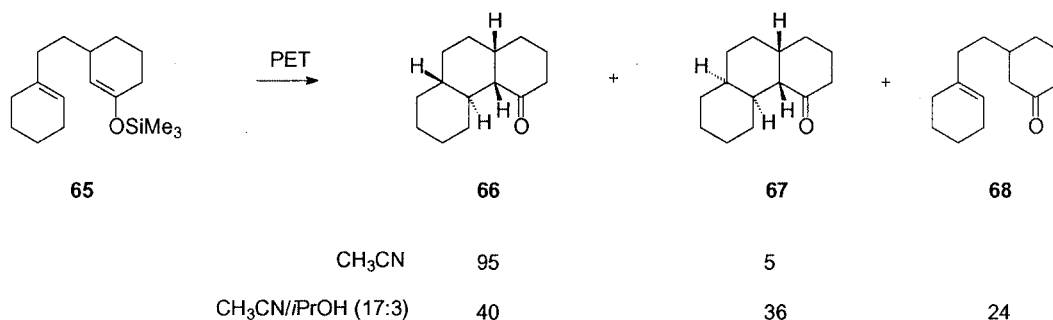
The rate constants were determined to be $k_{5\text{exo}} = 2 \times 10^9 \text{ s}^{-1}$ and $k_{6\text{exo}} = 2 \times 10^7 \text{ s}^{-1}$. Because of the highly stabilized double benzylic position in the product radical cations **63** and **64** and the accompanying enhanced reaction rate, we estimated the rate constants in our cyclization system to $k_{\text{cyc-cc}} = k_{\text{cyc-ct}} = \text{ca. } 2 \times 10^7 \text{ s}^{-1}$. These rates are about 10 times faster than those for the corresponding radical process.

The primary follow-up reaction, the mesolytic Si–O cleavage proceeds with a pseudo first-order rate constant of $k_{\text{desil}} = 2.3 \times 10^6 \text{ s}^{-1}$ in acetonitrile.^[60]

As a consequence, the rate constants involved in this reaction increases in the order $k_{\text{cyc-cc}} = k_{\text{cyc-ct}} > k_{\text{desil}} \gg k_{\text{sat}}$, which is in good agreement with our results.

If the cyclization reaction of the radical cation **13** proceeded under thermodynamic control, no *cis-cisoid* product **15c** would be formed because of the endothermic character of the cyclization process. If, on the other hand, the rate constant for the desilylation reaction were higher, the *cis-cisoid* product **15c** would not have been formed, because the α -carbonyl radical **32** cyclizes in only a *cis-transoid* fashion.

According to our model, the cyclization of **13** takes place to yield **22a** and **22b** intermediately; the back reaction then competes with desilylation. Desilylation may also take place at the noncyclized stage of **13**, because the ratio of rate constants of only 10 is not high enough to prevent this process from occurring. The resulting α -carbonyl radical **32** cyclizes in the described manner. A difference from the product dis-



Scheme 14

tribution cannot be observed; both pathways afford **15a** and **15b**.

The lack of *cis-cisoid* products from the cyclohexanone silyl enol ether radical cation **14** can be explained by a shorter lifetime of the corresponding cyclized radical cation **23b** and a faster ring opening reaction.

The saturation reaction of intermediate radicals **26a**, **26b**, and **27a** afforded a selectivity similar to that observed in the radical cyclization of iodo ketones **34** and **35**. Although the mechanism of the saturation process is not been understood fully,^[33] conformers of the cyclized radical will have a great influence of the diastereoselectivity. Therefore, an approach similar to the description of the radical saturation by tributyltin hydride seems to be an appropriate explanation.

If the rate constant for the saturation process increases, the product distribution will change significantly. This finding parallels experimental results obtained earlier in our group.^[28,29] PET oxidative cyclization of silyl enol ether **65** in acetonitrile afforded **66** and **67** in a 95:5 ratio (Scheme 14).

This ratio is in good agreement with our results from the cyclization of **12**. Cyclization in a mixture of 15% 2-propanol in acetonitrile resulted in a broader product spectrum. Uncyclized ketone **68** is produced in a considerable yield; it has not been observed at all in PET oxidative cyclization reactions previously. Furthermore, the selectivity in the saturation reaction vanishes, as is noticeable from the 40:36 ratio between **66** and **67**.

Originally, these results were interpreted as an enhanced mesolytic cleavage of the Si–O bond in the primary radical cation by the nucleophilic alcohol. The product distribution was thought to be the result of a cyclization of the resulting α -carbonyl radical.^[29]

The rate constant for the reaction between 2-propanol and benzylic trimethylsilyl radical cations had been determined as $k_{2\text{PrOH}} = 9.7 \times 10^5 \text{ L mol}^{-1} \text{ s}^{-1}$.^[61] A 15% mixture of 2-propanol has a concentration of ca. 2 M. This situation results in a pseudo-first-order rate constant of $k_{1\text{st}_{2\text{PrOH}}} = 1.94 \times 10^6 \text{ s}^{-1}$ and is very similar to the rate constant obtained in pure acetonitrile ($k_{\text{desil}} = 2.3 \times 10^6 \text{ s}^{-1}$). Therefore, the addition of 2-propanol should not enhance mesolytic Si–O cleavage.

In addition, 2-propanol undergoes hydrogen abstraction, which should open competing side-reactions. For the photochemically induced hydrogen abstraction of the triplet state of 4,4'-bipyridine from 2-propanol, a rate constant has been determined to be $k_{\text{bipy}} = 2.4 \times 10^5 \text{ L mol}^{-1} \text{ s}^{-1}$,^[61] the pseudo-first-order rate constant for a 15% mixture is $k_{1\text{st}_{\text{bipy}}} = 4.8 \times 10^5 \text{ s}^{-1}$. This rate is only ca. five times slower than the rate of desilylation and only ca. 50 times slower than the rate of cyclization (10^7 s^{-1}). Compared to the reaction rate for the saturation with tributyltin hydride ($k = 4 \times 10^3 \text{ s}^{-1}$), the hydrogen abstraction from 2-propanol is ca. 100 times faster. The saturation products at every stage of the reaction are shown in Scheme 14: **68** is the saturation product prior to cyclization, **67** is the product from saturation before the cyclized radicals were able to reach equilibrium (Figure 4), and **66** is the product observed originally after a slow saturation reaction.

The effect of adding 2-propanol is obviously different from the original interpretation. The rate of mesolytic cleavage is not altered by the addition of the alcohol, but the rate of radical saturation is enhanced drastically, resulting in a broader product spectrum. These findings give additional support for the mechanism of PET oxidative cyclization of silyl enol ethers that we have presented.

Conclusion

Using an independent synthetic approach to **15** and **16**, by radical cyclizations of iodo ketones **34** and **35**, accompanied by a variety of DFT calculations, we were able to conduct an in-depth study of the results of our PET-mediated oxidative cyclizations of silyl enol ethers **11** and **12**.

Radical cyclizations of iodo ketones **34** and **35** proceed with remarkable selectivity. The complete 6-*endo* selectivity of the cyclization can be explained by the stability of the intermediate α -carbonyl radical and a reversible 5-*exo* cyclization. We note that a simple correlation between 6-*endo* selectivity and radical cationic intermediates does not apply in this case.

The stereoselectivity of the ring closure and saturation steps can be explained by our results from DFT calcu-

lations, in combination with rate constants known in the literature, that support our model of a slow saturation process.

With these results, it was possible to describe also the radical cationic cyclization reaction. We could confirm that radical cations are indeed reactive intermediates in the cyclization step, although the contribution of a radical pathway could not be excluded.

The kinetics of the fundamental steps are of major importance, as is seen in the analysis of the PET reaction in an acetonitrile/2-propanol medium. Increasing the saturation rate leads to a completely different product spectrum. Combining the known rate constants with our own results from DFT calculations, we were able to present a comprehensive model for the PET-mediated oxidative cyclization of silyl enol ethers.

Experimental Section

General Remarks: ^1H NMR and ^{13}C NMR spectra were recorded at 300 K using either a Bruker DRX 500 or a Bruker Avance 600 spectrometer. Spectra were recorded in CDCl_3 or C_6D_6 ; chemical shifts were calibrated to the residual proton and carbon resonance of the solvent: CDCl_3 ($\delta_{\text{H}} = 7.26$ ppm, $\delta_{\text{C}} = 77.00$ ppm), C_6D_6 ($\delta_{\text{H}} = 7.20$ ppm, $\delta_{\text{C}} = 128.0$ ppm). IR spectra were recorded on a Perkin–Elmer 841 spectrometer. HRMS were recorded on an Autospec X (Vacuum Generators, Manchester). GC/MS were recorded on a Shimadzu GC 17A / QP 5050A equipped with a 5MS capillary column (Hewlett–Packard). Analytical thin-layer chromatography was performed on silica gel 60 F254 (Merck). Column chromatography was performed on silica gel MN60 (63–200 μm ; Macherey–Nagel). HPLC was performed on an RT 250–25 silica gel column [LiChrosorb Si60 (7 μm); Merck] using a Merck L6000 pump and an RI Bischoff 8110 detector (Bischoff). Photochemical reactions were performed using an RPR-100 Rayonet photochemical chamber reactor (Southern New England Ultraviolet Company) with RPR 4190-Å lamps that show an emission maximum at 419 ± 15 nm at half band width. All reactions were carried out under an atmosphere of argon. Starting materials and solvents were purified using standard laboratory techniques.^[62]

3-(1-Cyclohexenylethyl)-2-cyclohexen-1-one (18): *tert*-Butyllithium (10.0 mL, 17.0 mmol of a 1.7 M solution in pentane) was added to a solution of 2,2'-bipyridine (2 mg) in dry THF (80 mL) cooled to -78 °C and then a solution of 1-iodo-2-(1-cyclohexenyl)ethane **19**^{[32][63]} (1.75 g, 7.42 mmol) in dry THF (10 mL) was added dropwise. The reaction mixture was stirred for 1.5 h at -78 °C before a solution of 3-ethoxycyclohex-2-enone **21** (1.00 g, 7.13 mmol) in dry THF (10 mL) was added dropwise. After stirring for 1 h at -78 °C, the mixture was warmed to 0 °C and Et_2O (50 mL) and 2 N aq. HCl (50 mL) were added; the mixture was stirred for 20 min at room temp. before the layers were separated. The organic layer was washed successively with sat. aq. NaHCO_3 , water, and brine (50 mL each), dried (MgSO_4), filtered, and concentrated in vacuo. Purification by column chromatography (cyclohexane/ EtOAc , 90:10) and kugelrohr distillation afforded **18** (780 mg, 52%) as a colorless oil. NMR experiments: ^1H , H/H-COSY, ^{13}C , DEPT135, HMQC. ^1H NMR (500 MHz, CDCl_3): $\delta = 1.45$ – 1.53 (m, 2 H, H-6), 1.53 – 1.60 (m, 2 H, H-7), 1.84 – 1.90 (m, 2 H, H-8), 1.92 (m, 2 H, H-5), 1.93 (m, 2 H, H-2), 2.08 (dd, $J = 7.8$, 7.8 Hz, 2 H, H-9), 2.25 (m, 2 H, H-1), 2.27 (m, 2 H, H-10), 2.31 (m, 2 H, H-3), 5.37

(m, 1 H, H-4b), 5.82 (m, 1 H, H-4a) ppm. ^{13}C NMR (125.8 MHz, CDCl_3): $\delta = 22.26$ (t, C-6), 22.58 (t, C-2), 22.74 (t, C-7), 25.06 (t, C-5), 28.07 (t, C-8), 29.55 (t, C-1), 35.23 (t, C-9), 36.20 (t, C-10), 37.21 (t, C-3), 121.78 (d, 4b), 125.60 (d, 4a), 136.11 (s, 8a), 166.42 (s, 10a), 199.81 (s, C-4) ppm. GC/MS (EI, 70 eV): m/z (%) = 205 (0.4), 204 (2), 148 (13), 111 (10), 110 (100), 95 (36), 91 (14), 79 (23), 77 (15), 67 (50), 65 (14), 55 (42), 53 (29), 41 (38), 39 (23), 27 (16). GC/MS (CI, isobutane): m/z (%) = 206 (17), 205 (100). HRMS: calcd. for $\text{C}_{14}\text{H}_{20}\text{O}$ [M^+] $m/z = 204.1514$; found 204.1522; deviation, 3.9 ppm. $\text{C}_{14}\text{H}_{20}\text{O}$ (204.31): calcd. C 82.30, H 9.87; found C 81.89, H 9.73. IR (film): $\tilde{\nu} = 3326$, 2927 , 2660 , 1668 , 1625 , 1428 , 1372 , 1346 , 1324 , 1252 , 1191 , 1125 , 1079 , 1049 , 1008 , 964 , 917 , 885 , 859 , 837 , 800 , 755 cm^{-1} .

3-(1-Cyclohexenylethyl)-3-methyl-1-cyclohexenyl Trimethylsilyl Ether (12): In a flame-dried flask, copper(I) iodide (5.14 g, 27.0 mmol) was suspended in dry THF (100 mL) and the mixture was cooled in an ice/ NaCl slurry. Methylolithium (33.8 mL, 54.1 mmol of a 1.6 M solution in Et_2O) was added dropwise and the mixture was stirred until the yellow precipitate dissolved completely. The reaction mixture was cooled to -78 °C and a solution of trimethylsilyl chloride (2.93 g, 27.0 mmol) and 3-(1-cyclohexenylethyl)-2-cyclohexen-1-one (**18**) (2.77 g, 13.5 mmol) in dry THF (50 mL) was added dropwise. The cooled mixture was stirred for 2 h before being poured onto ice-cold 0.1 N aq. HCl (200 mL) and ice-cold pentane (250 mL) in a separating funnel. After shaking for a short time, the layers were separated and the organic layer was washed with ice-cold sat. aq. NaHCO_3 , dried (Na_2SO_4), and filtered. Concentration in vacuo afforded **12** (3.39 g, 86%) as a colorless oil. NMR experiments: ^1H , H/H-COSY, APT, HMQC. ^1H NMR (500 MHz, CDCl_3): $\delta = 0.175$ [s, 9 H, $\text{Si}(\text{CH}_3)_3$], 0.95 (s, 3 H, CH_3), 1.23 – 1.31 (m, 1 H, H-1), 1.28 – 1.39 (m, 2 H, H-10), 1.37 – 1.44 (m, 1 H, H-1), 1.50 – 1.57 (m, 2 H, H-6), 1.57 – 1.64 (m, 2 H, H-7), 1.61 – 1.68 (m, 2 H, H-2), 1.80 – 1.92 (m, 2 H, H-9), 1.89 – 1.94 (m, 2 H, H-8), 1.91 – 1.94 (m, 2 H, H-3), 1.95 – 2.00 (m, 2 H, H-5), 4.65 (dd, $J = 1.5$, 1.5 Hz, 1 H, H-4a), 5.38 (m, 1 H, H-4b) ppm. ^{13}C NMR (125.8 MHz, CDCl_3): $\delta = 0.13$ [q, $\text{Si}(\text{CH}_3)_3$], 19.62 (t, C-2), 22.57 (t, C-6), 23.06 (t, C-7), 25.24 (t, C-5), 28.02 (q, Me), 28.52 (t, C-8), 29.86 (t, C-3), 32.76 (t, C-9), 34.43 (s, C-10a), 34.46 (t, C-1), 41.64 (t, C-10), 114.45 (d, C-4a), 120.08 (d, C-4b), 138.63 (s, C-8a), 149.22 (s, C-4) ppm. GC/MS (EI, 70 eV): m/z (%) = 293 (0.4), 292 (1), 184 (15), 183 (100), 73 (39). HRMS: calcd. for $\text{C}_{18}\text{H}_{32}\text{OSi}$ [M^+], $m/z = 292.2222$; found 292.2225; deviation, 0.9 ppm. $\text{C}_{18}\text{H}_{32}\text{OSi}$ (292.54): calcd. C 73.90, H 11.03; found C 74.63, H 11.30. IR (film): $\tilde{\nu} = 2935$, 2841 , 1662 , 1453 , 1365 , 1341 , 1263 , 1251 , 1207 , 1193 , 1164 , 1134 , 1102 , 1058 , 964 , 936 , 909 , 889 , 841 , 801 , 753 , 686 cm^{-1} .

PET Cyclization of 3-(1-Cyclohexenylethyl)-3-methyl-1-cyclohexenyl Trimethylsilyl Ether (12): A solution of **12** (130 mg, 0.44 mmol), DCN (42 mg, 0.42 mmol), and decane (66 μL) in dry acetonitrile (66 mL) was filled into irradiation tubes (11 mL each, pyrex glass, 12 mm diameter), degassed with argon for 20 min, and irradiated with light (350 nm) until complete consumption of the starting material. The reaction mixture was concentrated in vacuo and the residue was subjected to column chromatography (cyclohexane/ EtOAc , 90:10). The diastereoisomers were separated by HPLC (cyclohexane/ EtOAc , 85:15) affording (4a*R**,4b*S**,8a*R**,10a*S**)-10a-methyl dodecahydro-4(1*H*)-phenanthrenone (**16a**) (55.0 mg, 56%) and (4a*R**,4b*S**,8a*S**,10a*S**)-10a-methyl dodecahydro-4(1*H*)-phenanthrenone (**16b**) (5.5 mg, 5.6%) in 62% combined isolated yield. The diastereoisomeric ratio was determined by GC directly from the reaction mixture (**16a**:**16b**, 90:10).

(4aR*,4bS*,8aR*,10aS*)-10a-Methyldodecahydro-4(1H)-phenanthrene (16a): NMR experiments: ^1H , H/H-COSY, APT, HMQC, HMBC, NOESY. ^1H NMR (500 MHz, CDCl_3): δ = 0.81 (d, J = 0.86 Hz, 3 H, CH_3), 0.82 (dddd, J = 3.9, 3.9, 11.2, 11.2, 11.2 Hz, 1 H, H-8a), 0.83 (dddd, J = 3.5, 3.5, 11.4, 11.4, 11.4 Hz, 1 H, H-5ax), 0.97 (dddd, J = 3.9, 11.3, 13.0, 13.0 Hz, 1 H, H-8ax), 1.01 (dddd, J = 1.7, 1.7, 2.4, 4.3, 13.7 Hz, 1 H, H-1eq), 1.10 (dddd, J = 3.4, 3.4, 12.7, 12.7, 12.7 Hz, 1 H, H-6ax), 1.13 (dddd, J = 3.4, 3.4, 12.3, 12.3, 12.3 Hz, 1 H, H-7ax), 1.20 (ddd, J = 4.4, 13.3, 13.3 Hz, 1 H, H-10ax), 1.27 (dddd, J = 1.5, 3.3, 3.3, 3.3, 13.4 Hz, 1 H, H-5eq), 1.31 (dddd, J = 3.5, 11.4, 13.3, 13.3 Hz, 1 H, H-9ax), 1.38 (dddd, J = 3.5, 10.9, 10.9, 11.1 Hz, 1 H, H-4b), 1.39 (dddd, J = 2.6, 4.5, 4.5, 13.2 Hz, 1 H, H-9eq), 1.479 (ddd, J = 3.1, 3.1, 13.2 Hz, 1 H, H-10eq), 1.595 (dddd, J = 3.2, 3.2, 3.2, 3.2, 12.9 Hz, 1 H, H-8eq), 1.61 (dddd, J = 3.2, 3.2, 3.2, 3.2, 12.5 Hz, 1 H, H-7eq), 1.63 (ddd, J = 1.5, 1.5, 11.4 Hz, 1 H, H-4a), 1.64 (dddd, J = 1.80, 3.2, 3.2, 3.2, 3.2, 11.4 Hz, 1 H, H-6eq), 1.79 (dddd, J = 4.7, 4.7, 13.7, 13.7 Hz, 1 H, H-2ax), 1.89 (dddd, J = 1.6, 2.1, 4.9, 7.3, 13.7 Hz, 1 H, H-2eq), 2.07 (dddd, J = 1.6, 1.6, 1.6, 4.9, 13.7 Hz, 1 H, H-3eq), 2.15 (ddd, J = 4.9, 13.7, 13.7 Hz, 1 H, H-1ax), 2.31 (ddd, J = 7.3, 13.7, 13.7 Hz, 1 H, H-3ax) ppm. ^{13}C NMR (125.8 MHz, CDCl_3): δ = 22.52 (t, C-2), 25.99 (t, C-7), 26.29 (t, C-6), 27.77 (q, Me), 29.06 (t, C-9), 29.43 (t, C-1), 30.69 (t, C-5), 33.87 (t, C-8), 37.35 (t, C-3), 37.95 (s, C-10a), 39.37 (t, C-10), 41.27 (d, C-4b), 42.11 (d, C-8a), 65.79 (d, C-4a), 215.69 (s, C-4) ppm. GC/MS (EI, 70 eV): m/z (%) = 221 (5), 220 (14), 205 (25), 202 (11), 111 (100), 109 (12), 108 (18), 95 (26), 93 (15), 91 (12), 81 (18), 79 (22), 67 (26), 55 (22), 41 (26). GC/MS (CI, isobutane): m/z (%) = 222 (14), 221 (100), 220 (4), 203 (3), 114 (3). HRMS: calcd. for $\text{C}_{15}\text{H}_{24}\text{O}$ [M^+], m/z = 220.1827; found 220.1826; deviation, 0.7 ppm. $\text{C}_{15}\text{H}_{24}\text{O}$ (220.35): calcd. C 81.76, H 10.98; found C 81.87, H 11.24. IR (film): $\tilde{\nu}$ = 2963, 2932, 2860, 2298, 1698, 1453, 1374, 1345, 1301, 1273, 1254, 1230, 1202, 1153, 1123, 1107, 1063, 1040, 974, 961, 904, 886, 852, 837, 786, 776, 730 cm^{-1} .

(4aR*,4bS*,8aS*,10aS*)-10a-Methyldodecahydro-4(1H)-phenanthrene (16b): NMR experiments: ^1H , H/H-COSY, ^{13}C , DEPT135, HMQC, HMBC, NOESY. ^1H NMR (500 MHz, CDCl_3): δ = 0.89 (s, 3 H, CH_3), 0.99 (dddd, J = 1.4, 1.4, 2.7, 4.3, 13.8 Hz, 1 H, H-1eq), 1.13–1.46 (m, 9 H, H-5, H-5, H-6, H-6, H-7, H-8eq, H-9, H-10, H-10), 1.52 (dddd, J = 3.6, 13.0, 13.0, 13.0 Hz, 1 H, H-8ax), 1.68–1.77 (m, 2 H, H-7, H-8a), 1.83 (dddd, J = 4.7, 4.7, 13.6, 13.6 Hz, 1 H, H-2ax), 1.83–1.95 (m, 2 H, H-2eq, H-9), 2.10 (dddd, J = 1.7, 1.7, 1.7, 4.9, 13.8 Hz, 1 H, H-3eq), 2.16 (dddd, J = 3.7, 3.7, 3.7, 12.4 Hz, 1 H, H-4b), 2.266 (ddd, J = 5.0, 13.7, 13.7 Hz, 1 H, H-1ax), 2.36 (ddd, 1.5, 1.5, 12.4 Hz, 1 H, H-4a), 2.38 (ddd, J = 7.4, 13.7, 13.7 Hz, 1 H, H-3ax) ppm. ^{13}C NMR (500 MHz, CDCl_3): δ = 19.66 (t, C-6), 22.38 (t, C-2), 25.39 (t, C-8), 26.41 (t, C-7), 27.14 (t, C-9), 28.20 (q, CH_3), 28.57 (t, C-5), 28.79 (t, C-1), 33.86 (t, C-10), 34.38 (d, C-4b), 35.76 (d, C-8a), 37.06 (t, C-3), 37.81 (s, C-10a), 56.22 (d, C-4a), 216.43 (s, C-4) ppm. GC/MS (EI, 70 eV): m/z (%) = 221 (2), 220 (8), 112 (100), 111 (100), 109 (11), 108 (13), 95 (18), 93 (11), 91 (12), 81 (11), 79 (19), 67 (16), 55 (15), 41 (20). GC/MS (CI, isobutane): m/z (%) = 222 (13), 221 (100), 220 (3), 203 (5), 111 (4). HRMS: calcd. for $\text{C}_{15}\text{H}_{24}\text{O}$ [M^+], m/z 220.1827; found 220.1824; deviation, 1.5 ppm. $\text{C}_{15}\text{H}_{24}\text{O}$ (220.35): calcd. C 81.76, H 10.98; found C 81.20, H 10.98. IR (film): $\tilde{\nu}$ = 2963, 2931, 2869, 2852, 2673, 2328, 1846, 1796, 1774, 1753, 1740, 1729, 1692, 1546, 1453, 1443, 1427, 1383, 1345, 1309, 1286, 1261, 1240, 1210, 1156, 1123, 1071, 1054, 989, 953, 898, 876, 830, 820, 780, 730, 665 cm^{-1} .

3-(1-Cyclohexenylethyl)-2-iodo-3-methyl-1-cyclohexanone (30): Freshly prepared *N*-iodosuccinimide (773 mg, 3.42 mmol) in dry

THF was added to a THF solution (70 mL) of 3-(1-cyclohexenylethyl)-3-methyl-1-cyclohexenyl trimethylsilyl ether (**12**) (1.00 g, 3.42 mmol) in a flask wrapped with aluminum foil. After stirring for 1 h, sat. aq. $\text{Na}_2\text{S}_2\text{O}_3$ (100 mL) and Et_2O (80 mL) were added. The layers were separated and the organic layer was dried (MgSO_4) and concentrated in vacuo to afford **30** (911 mg, 77%) as a yellowish, light-sensitive oil. NMR experiments: ^1H , H/H-COSY, ^{13}C , DEPT135. ^1H NMR (500 MHz, CDCl_3): δ = 1.06 (s, 3 H, Me), 1.11 (s, 3 H, Me), 1.35–1.68 (m, 17 H), 1.74–2.06 (m, 17 H), 2.23–2.34 (m, 2 H), 3.18–3.28 (m, 1 H), 3.33–3.44 (m, 1 H), 4.261 (dd, J = 1.6, 1.6 Hz, 1 H, H-4a), 4.43 (dd, J = 1.4, 1.4 Hz, 1 H, H-4a), 5.39 (m, 1 H, H-4b), 5.43 (m, 1 H, H-4b) ppm. ^{13}C NMR (500 MHz, CDCl_3): δ = 19.70 (q, Me), 21.01/21.18 (t, C-2), 22.38/22.45 (t, C-6), 22.92/22.97 (t, C-7), 25.19/25.21 (t, C-5), 27.26 (q, Me), 28.42/28.51 (t, C-8), 31.01/31.17 (t), 32.56/32.65 (t, C-9), 34.74 (t), 35.04 (t), 35.32 (t), 39.74 (s, C-10a), 40.56 (s, C-10a), 41.54 (t), 47.17 (d, C-4a), 49.31 (d, C-4a), 121.20/121.43 (d, C-4b), 137.06/137.18 (s, C-8a), 205.87/205.37 (s, C-4) ppm.

Derivatization for ESI-MS: A TLC-plate spotted with **30** was dipped into a solution of Girard's reagent T [*N*-(hydrazinocarbonylmethyl)trimethylammonium chloride (4 mg/mL) in 0.1% aq. formic acid] and dried for 5 min in an oven at 80 °C. The plate was then subjected to ESI-MS. MS (ESI): m/z = 460 [M^+], 333 [$\text{M} - \text{I}]^+$, 350, 332 [$\text{M} - \text{I} - \text{I}]^+$, 132. MS/MS (ESI): 459 [$\text{M} - \text{I}]^+$, 333 [$\text{M} - \text{I}]^+$, 274 [$\text{M} - \text{I} - \text{NMe}_3]^+$, 224 [$\text{M} - \text{I} - \text{C}_8\text{H}_{13}]^+$.

Radical Cyclization of 3-(1-Cyclohexenylethyl)-2-iodo-3-methyl-1-cyclohexanone (30): AIBN (16 mg, 0.1 mmol) was added to a solution of 3-(1-cyclohexenylethyl)-2-iodo-3-methyl-1-cyclohexanone (**30**) (519 mg, 1.50 mmol) and tributyltin hydride (437 mg, 1.5 mmol) in dry benzene (400 mL). The solution was stirred for 4 h under reflux and then concentrated in vacuo. The residue was purified by column chromatography (cyclohexane/ EtOAc , 90:10) to afford a mixture of **16a** and **16b** (109 mg, 33%). The diastereoisomeric ratio was determined by GC directly from the reaction mixture (**16a**:**16b**, 90:10).

3-(1-Cyclohexenylethyl)-2-cyclopenten-1-one (17): As described for the synthesis of **18**, **17** (660 mg, 47%) was synthesized from 1-iodo-2-(1-cyclohexenyl)ethane (**19**) (1.73 g, 7.33 mmol) and 3-ethoxycyclopent-2-enone (**20**)^[64–67] (1.11 g, 8.80 mmol) after purification by column chromatography (cyclohexane/ EtOAc , 90:10) and kugelrohr distillation. NMR experiments: ^1H , H/H-COSY, APT, HMQC. ^1H NMR (500 MHz, CDCl_3): δ = 1.43–1.57 (m, 2 H, H-8), 1.58–1.62 (m, 2 H, H-7), 1.82–1.90 (m, 2 H, H-6), 1.90–1.97 (m, 2 H, H-9), 2.16 (t, J = 7.8 Hz, 2 H, H-5), 2.30–2.37 (m, 2 H, H-2), 2.47 (t, J = 7.8 Hz, 2 H, H-4), 2.51–2.57 (m, 2 H, H-3), 5.38 (m, 1 H, H-9a), 5.90 (m, 1 H, H-9b) ppm. ^{13}C NMR (125.8 MHz, CDCl_3): δ = 22.23 (t, C-8), 22.70 (t, C-7), 25.01 (t, C-9), 28.06 (t, C-8), 31.42 (t, C-3), 31.51 (t, C-4), 35.11 (t, C-2/5), 35.14 (t, C-2/5), 121.82 (d, C-9a), 129.37 (d, C-9b), 135.89 (s, C-5a), 182.87 (s, C-3a), 210.04 (s, C-1) ppm. GC/MS (EI, 70 eV): m/z (%) = 191 (0.8), 190 (3), 148 (55), 133 (17), 97 (14), 96 (100), 95 (90), 94 (10), 93 (16), 91 (23), 81 (13), 79 (39), 77 (26), 67 (92), 66 (18), 65 (26), 55 (58), 53 (46), 52 (11), 51 (15), 41 (69), 39 (46), 29 (13), 28 (10), 27 (30). GC/MS (CI, isobutane): m/z (%) = 192 (13), 191 (100). HRMS: calcd. for $\text{C}_{13}\text{H}_{18}\text{O}$ [M^+], m/z = 190.1358; found 190.1351; deviation, 3.4 ppm. IR (film): $\tilde{\nu}$ = 2923, 2859, 2838, 1714, 1677, 1614, 1438, 1409, 1336, 1268, 1229, 1186, 1135, 1079, 1049, 973, 918, 840, 801 cm^{-1} .

3-(1-Cyclohexenylethyl)-3-methyl-1-cyclopentenyl Trimethylsilyl Ether (11): As described for the synthesis of **12**, **11** (4.50 mg, 93%) was synthesized as a colorless oil from 3-(1-cyclohexenylethyl)-2-

cyclopenten-1-one (**17**) (3.34 g, 17.5 mmol). NMR experiments: ^1H , H/H-COSY, APT, HMQC. ^1H NMR (500 MHz, CDCl_3): δ = 0.20 [s, 9 H, $\text{Si}(\text{CH}_3)_3$], 1.02 (s, 3 H, CH_3), 1.34–1.46 (m, 2 H, H-4), 1.51–1.57 (m, 2 H, H-8), 1.55 (ddd, J = 6.0, 9.1, 12.7 Hz, 1 H, H-3), 1.57–1.63 (m, 2 H, H-7), 1.71 (ddd, J = 5.8, 8.9, 12.7 Hz, 1 H, H-3), 1.81–1.91 (m, 2 H, H-5), 1.88–1.94 (m, 2 H, H-6), 1.94–2.00 (m, 2 H, H-9), 2.26 (dddd, J = 1.6, 5.8, 8.7, 15.9 Hz, 1 H, H-2), 2.31 (dddd, J = 1.6, 5.8, 8.9, 15.9 Hz, 1 H, H-2), 4.49 (dd, J = 1.6, 1.6 Hz, 1 H, H-9b), 5.38 (m, 1 H, H-9a) ppm. ^{13}C NMR (125.8 MHz, CDCl_3): δ = -0.01 [q, $\text{Si}(\text{CH}_3)_3$], 22.60 (t, C-8), 23.07 (t, C-7), 25.25 (t, C-9), 28.02 (q, Me), 28.58 (t, C-6), 33.22 (t, C-2), 33.62 (t, C-5), 34.89 (t, C-3), 41.00 (t, C-4), 44.94 (s, C-3a), 112.23 (d, C-9b), 120.00 (d, C-9a), 138.66 (s, C-5a), 152.86 (s, C-1) ppm. GC/MS (EI, 70 eV): m/z (%) = 279 (1), 278 (5), 170 (27), 169 (100), 75 (12), 73 (48), 45 (12). HRMS: calcd. for $\text{C}_{17}\text{H}_{30}\text{OSi}$ [M^+], m/z 278.2067; found 278.2067. $\text{C}_{17}\text{H}_{30}\text{OSi}$ (278.51): calcd. C 73.31, H 10.86; found C 71.82, H 10.54. IR (film): $\tilde{\nu}$ = 2930, 2862, 1747, 1716, 1644, 1453, 1439, 1371, 1341, 1308, 1252, 1197, 1135, 1074, 1047, 997, 931, 871, 844, 803, 757, 689, 665 cm^{-1} .

PET Cyclization of 3-(1-Cyclohexenylethyl)-3-methyl-1-cyclopentenyl Trimethylsilyl Ether (11**) Using DCN as a Sensitizer:** A solution of 3-(1-cyclohexenylethyl)-3-methyl-1-cyclopentenyl trimethylsilyl ether (**11**) (196 mg, 0.95 mmol) and DCN (50 mg, 0.28 mmol) in dry acetonitrile (55 mL) was filled into irradiation tubes (11 mL each, pyrex glass, 12 mm diameter), degassed with argon for 20 min, and irradiated with light (350 nm) until complete consumption of the starting material occurred. The reaction mixture was concentrated in vacuo and the residue was subjected to column chromatography (cyclohexane/EtOAc, 90:10) to afford a mixture of (3a*R**,5a*R**,9a*S**,9b*R**)-3a-methyldecacyhydro-1*H*-cyclopenta[*a*]naphthalen-1-one (**15a**), (3a*R**,5a*S**,9a*S**,9b*R**)-3a-methyldecacyhydro-1*H*-cyclopenta[*a*]naphthalen-1-one (**15b**), and (3a*R**,5a*S**,9a*R**,9b*R**)-3a-methyldecacyhydro-1*H*-cyclopenta[*a*]naphthalen-1-one (**15c**) (64 mg, 33%). The diastereoisomeric ratio was determined by GC directly from the reaction mixture (**15a**/**15b**/**15c** = 41:31:28). Isomer **15c** was separated by HPLC (cyclohexane/EtOAc, 92.5:7.5); **15a** and **15b** were isolated by preparative GC.

(3a*R,5a*R**,9a*S**,9b*R**)-3a-Methyldecacyhydro-1*H*-cyclopenta[*a*]naphthalen-1-one (**15a**):** NMR experiments: ^1H , H/H-COSY, APT, HMQC, HMBC, NOESY. ^1H NMR (500 MHz, C_6D_6): δ = 0.60 (dddd, J = 3.3, 3.3, 10.5, 11.5, 11.5 Hz, 1 H, H-5a), 0.704 (ddd, J = 3.3, 11.0, 11.0, 11.0 Hz, 1 H, H-9a), 0.73 (d, J = 0.9 Hz, 3 H, CH_3), 0.85 (dddd, J = 3.7, 11.4, 12.8, 12.8 Hz, 1 H, H-6ax), 0.90 (ddd, J = 3.4, 11.3, 12.8, 12.8 Hz, 1 H, H-9ax), 1.00 (dddd, J = 1.4, 5.7, 5.7, 13.0 Hz, 1 H, H_a-3), 1.02 (dddd, J = 4.1, 13.1, 13.1, 13.1 Hz, 1 H, H-5ax), 1.09 (dddd, J = 3.3, 3.3, 12.8, 12.8, 12.8 Hz, 1 H, H-7ax), 1.16 (dddd, J = 3.4, 3.4, 12.8, 12.8, 12.8 Hz, 1 H, H-8ax), 1.18 (ddd, J = 4.5, 13.2, 13.2 Hz, 1 H, H-4ax), 1.26 (ddd, J = 2.8, 2.8, 4.3, 13.9 Hz, 1 H, H-5eq), 1.33 (dd, J = 1.5, 11.1 Hz, 1 H, H-9b), 1.34 (ddd, J = 2.5, 4.0, 13.3 Hz, 1 H, H-4eq), 1.54 (dddd, J = 1.8, 3.3, 3.3, 3.3, 13.03 Hz, 1 H, H-6eq), 1.64 (dddd, J = 1.72, 3.3, 3.3, 3.3, 12.7 Hz, 1 H, H-8eq), 1.70 (dddd, J = 1.8, 3.3, 3.3, 3.3, 12.8 Hz, 1 H, H-7eq), 1.79 (ddd, J = 10.4, 10.4, 12.9 Hz, 1 H, H_i-3), 2.06 (ddd, J = 5.6, 10.4, 19.7 Hz, 1 H, H-2), 2.11 (ddd, J = 5.6, 9.9, 19.7 Hz, 1 H, H-2), 2.31 (dddd, J = 1.7, 3.3, 3.3, 3.3, 13.3 Hz, 1 H, H-9eq) ppm. ^{13}C NMR (150.96 MHz, C_6D_6): δ = 26.53 (t, C-8), 26.73 (t, C-7), 29.28 (t, C-3), 29.38 (q, CH_3), 29.53 (t, C-5), 31.09 (t, C-9), 34.42 (t, C-6), 34.48 (t, C-2), 35.03 (t, C-4), 38.56 (s, C-3a), 39.86 (d, C-9a), 40.97 (d, C-5a), 61.97 (d, C-9b), 217.15 (s, C-1) ppm. GC/MS (EI, 70 eV): m/z (%) = 207 (4), 206 (28), 191 (23), 108 (37), 107 (15), 98 (17),

97 (100), 96 (16), 95 (17), 93 (17), 91 (12), 81 (39), 79 (26), 77 (10), 67 (28), 55 (30), 53 (17), 41 (33), 39 (13), 29 (14), 28 (10), 27 (14). GC/MS (CI, isobutane): m/z (%) = 208 (25), 207 (100), 206 (29), 189 (18). HRMS: calcd. for $\text{C}_{14}\text{H}_{22}\text{O}$ [M^+], m/z 206.1671; found 206.1662; deviation, 4.4 ppm. IR (film): $\tilde{\nu}$ = 2923, 2857, 2243, 1739, 1449, 1412, 1379, 1253, 1217, 1173, 1156, 1141, 1121, 1088, 1059, 1035, 988, 919, 857, 835, 665 cm^{-1} .

(3a*R,5a*S**,9a*S**,9b*R**)-3a-Methyldecacyhydro-1*H*-cyclopenta[*a*]naphthalen-1-one (**15b**):** NMR experiments: ^1H ; H/H-COSY; APT; HMQC; HMBC at T = 370 and 213 K; ^1H NMR spectra in steps of 10 K between T = 213 and 370 K; NOESY at T = 370 K. ^1H NMR (600 MHz, $\text{C}_2\text{D}_2\text{Cl}_4$, T = 370 K): δ = 1.16 (s, 3 H, Me), 1.22–1.47 (m, 10 H), 1.51 (ddd, J = 9.2, 9.2, 12.9 Hz, 1 H, H-3), 1.58–1.70 (m, 2 H, H-5, H-8), 1.67 (dd, J = 1.1, 4.1 Hz, 1 H, H-9b), 1.71 (dddd, J = 3.5, 3.5, 10.4, 10.4, 10.4 Hz, 1 H, H-9ax), 1.76 (ddd, J = 6.6, 6.6, 13.0 Hz, 1 H, H-3), 2.04 (dddd, J = 4.3, 4.3, 4.3, 10.5 Hz, 1 H, H-9a), 2.18 (ddd, J = 6.9, 9.1, 14.7 Hz, 1 H, H-2), 2.20 (ddd, J = 6.9, 9.1, 14.7 Hz, 1 H, H-2) ppm. ^{13}C NMR (150.96 MHz, $\text{C}_2\text{D}_2\text{Cl}_4$, T = 370 K): δ = 22.95 (t, C-7), 23.98 (t, C-5), 25.72 (t, C-8), 28.02 (t, C-9), 28.83 (q, Me), 30.65 (t, C-6), 33.89 (t, C-4), 34.08 (t, C-3), 34.77 (d, C-5a), 34.94 (d, C-9a), 35.03 (t, C-2), 38.38 (s, C-3a), 60.23 (d, C-9b), 219.83 (s, C-1) ppm. ^1H NMR (600 MHz, CD_2Cl_2 , T = 213 K): δ = 1.01 (dddd, J = 3.4, 3.4, 3.4, 13.3 Hz, 1 H, H-5eq), 1.10–1.38 (m, 7 H), 1.194 (s, 3 H, Me), 1.38–1.46 (m, 2 H), 1.50–1.65 (m, 4 H), 1.61 (m, 1 H, H-9b), 1.69 (dddd, J = 3.2, 13.2, 13.2, 13.2 Hz, 1 H, H-5ax), 2.08 (ddd, J = 4.1, 4.1, 13.4 Hz, 1 H, H-9a), 2.13–2.25 (m, 2 H, H-2) ppm. ^{13}C NMR (150.96 MHz, CD_2Cl_2 , T = 213 K): δ = 20.54 (t), 21.31 (t, C-5), 26.59 (t), 26.82 (t), 27.24 (q, Me), 31.32 (t), 33.38 (d, C-5a), 33.64 (t, C-4), 34.28 (t, C-3), 34.38 (d, C-9a), 34.44 (t, C-2), 37.65 (s, C-3a), 61.46 (d, C-9b), 221.21 (s, C-1) ppm. GC/MS (EI, 70 eV): m/z (%) = 207 (2), 206 (13), 191 (12), 97 (100), 41 (13). GC/MS (CI, isobutane): m/z (%) = 208 (15), 207 (100), 206 (24), 205 (19), 189 (23). HRMS: calcd. for $\text{C}_{14}\text{H}_{22}\text{O}$ [M^+], m/z = 206.1671; found 206.16668; deviation, 0.78 ppm. IR (film): $\tilde{\nu}$ = 2928, 2863, 2667, 1736, 1452, 1410, 1381, 1350, 1286, 1264, 1202, 1181, 1163, 1147, 1111, 1091, 1073, 1023, 994, 953, 904, 870, 799 cm^{-1} .

(3a*R,5a*S**,9a*R**,9b*R**)-3a-Methyldecacyhydro-1*H*-cyclopenta[*a*]naphthalen-1-one (**15c**):** NMR experiments: ^1H , H/H-COSY, ^{13}C , DEPT135, HMQC, HMBC. ^1H NMR (600 MHz, C_6D_6): δ = 0.85 (dddd, J = 3.8, 11.0, 13.0, 13.0 Hz, 1 H, H-6ax), 0.92 (d, J = 0.9 Hz, 3 H, CH_3), 0.99 (dddd, J = 3.6, 11.2, 13.3, 13.3 Hz, 1 H, H-5ax), 1.02 (ddd, J = 2.2, 3.7, 13.5 Hz, 1 H, H-4eq), 1.07 (dddd, J = 0.8, 3.7, 13.6, 13.6 Hz, 1 H, H-4ax), 1.16 (dddd, J = 3.3, 3.3, 11.2, 13.0, 13.0 Hz, 1 H, H-5a), 1.18 (ddd, J = 10.4, 10.4, 12.6 Hz, 1 H, H-3), 1.18 (dddd, J = 3.7, 3.7, 13.0, 13.0, 13.0 Hz, 1 H, H-8ax), 1.19 (m, 1 H, H-9a), 1.29 (ddd, J = 2.0, 8.9, 12.6 Hz, 1 H, H-3), 1.29 (m, 1 H, H-5eq), 1.37 (dddd, J = 3.6, 3.6, 13.1, 13.1, 13.1 Hz, 1 H, H-7ax), 1.42 (ddd, J = 1.4, 2.3, 3.8 Hz, 1 H, H-9b), 1.52 (dddd, J = 1.8, 3.3, 3.3, 3.3, 13.4 Hz, 1 H, H-9eq), 1.60 (dddd, J = 1.8, 3.3, 3.3, 3.3, 12.9 Hz, 1 H, H-6eq), 1.69 (dddd, J = 1.7, 3.3, 3.3, 3.3, 13.0 Hz, 1 H, H-7eq), 1.88 (dddd, J = 1.8, 3.3, 3.3, 3.3, 12.7 Hz, 1 H, H-8eq), 1.92 (ddd, J = 1.3, 2.0, 10.0, 19.2 Hz, 1 H, H-2), 2.00 (ddd, J = 8.8, 10.5, 19.2 Hz, 1 H, H-2), 2.79 (dddd, J = 3.7, 11.8, 13.4, 13.4 Hz, 1 H, H-9ax) ppm. ^{13}C NMR (150.96 MHz, C_6D_6): δ = 24.86 (q, CH_3), 26.63 (t, C-7), 27.74 (t, C-8), 29.16 (t, C-9), 30.65 (t, C-5), 33.14 (t, C-4), 34.50 (t, C-3), 34.59 (t, C-6), 35.16 (t, C-2), 37.69 (d, C-5a), 39.65 (s, C-3a), 40.12 (d, C-9a), 59.44 (d, C-9b), 216.90 (s, C-1) ppm. GC/MS (EI, 70 eV): m/z (%) = 207 (2), 206 (10), 97 (100), 79 (10), 67 (10), 55 (11), 41 (14). GC/MS (CI, isobutane): m/z (%) = 207 (100),

206 (26), 205 (21), 192 (12), 191 (11), 189 (74). HRMS: calcd. for $C_{14}H_{22}O$ [M^+], $m/z = 206.1671$; found 206.1663; deviation, 3.6 ppm. IR (film): $\tilde{\nu} = 2913, 2854, 2822, 2668, 2307, 1813, 1735, 1449, 1407, 1379, 1344, 1317, 1288, 1261, 1229, 1199, 1169, 1127, 1047, 986, 954, 942, 887, 862, 842, 798\text{ cm}^{-1}$.

PET Cyclization of 3-(1-Cyclohexenylethyl)-3-methyl-1-cyclopentenyltrimethylsilyl Ether (11) using DCA/Phenanthrene: A solution of 3-(1-cyclohexenylethyl)-3-methyl-1-cyclopentenyl trimethylsilyl ether (**11**) (521 mg, 1.87 mmol), DCA (60 mg, 0.26 mmol), and phenanthrene (360 mg, 2.0 mmol) in dry acetonitrile (66 mL) was filled into irradiation tubes (11 mL each, pyrex glass, 12 mm diameter), degassed with argon for 20 min, and irradiated with light (420 nm) until complete consumption of the starting material occurred. The reaction mixture was concentrated in vacuo and the residue was subjected to column chromatography (cyclohexane/EtOAc, 90:10) to afford a mixture of **15a**, **15b**, and **15c** (167 mg, 43%). The diastereoisomeric ratio was determined by GC directly from the reaction mixture (**15a/15b/15c**, 41:31:28).

3-(1-Cyclohexenylethyl)-2-iodo-3-methyl-1-cyclopentanone (29): As described for the synthesis of **30**, **29** (285 mg, 83%) was synthesized as a yellowish, light-sensitive oil from 3-(1-cyclohexenylethyl)-3-methyl-1-cyclopentenyl trimethylsilyl ether (**11**). NMR experiments: ^1H , H/H-COSY, ^{13}C . ^1H NMR (500 MHz, CDCl_3): $\delta = 1.11$ (s, 3 H, Me), 1.14 (s, 3 H, Me), 1.44–1.67 (m, 13 H), 1.74 (dddd, $J = 1.4, 3.1, 9.0, 13.0$ Hz, 1 H), 1.84–2.08 (m, 15 H), 2.25 (dddd, $J = 1.2, 8.8, 8.8, 19.7$ Hz, 1 H), 2.28–2.38 (m, 2 H), 2.44 (dddd, $J = 0.6, 3.1, 9.9, 19.8$ Hz, 1 H), 4.22 (dd, $J = 1.5, 1.5$ Hz, 1 H, H-9b), 4.48 (dd, $J = 0.8, 0.8$ Hz, 1 H, H-9b), 5.41 (m, 1 H, H-9a), 5.44 (m, 1 H, H-9a) ppm. ^{13}C NMR (500 MHz, CDCl_3): $\delta = 20.78$ (q, Me), 22.39/22.44 (t, C-8), 22.91/22.95 (t, C-7), 25.18/25.19 (t, C-9), 25.69 (q, Me), 28.46/28.49 (t, C-6), 31.40, 32.40/32.42, 32.74/32.78, 32.89, 40.83, 42.17, 42.51, 44.66, 45.73, 121.16/121.39 (d, C-9a), 137.03/137.16 (s, C-5a), 211.51/211.53 (s, C-1) ppm. Derivatization for ESI-MS: A TLC-plate spotted with **29** was dipped into a solution of Girard's reagent T [N -(hydrazinocarbonylmethyl)trimethylammonium chloride (4 mg/mL) in 0.1% aq. formic acid] and dried for 5 min in an oven at 80 °C. The plate was then subjected to ESI-MS. MS (ESI): $m/z = 478, 446$ [M^+], 355, 336 [$M - C_8H_{14}$] $^+$, 318 [$M - I - 1$] $^+$, 172, 132.

Radical Cyclization of 3-(1-Cyclohexenylethyl)-2-iodo-3-methyl-1-cyclopentanone (29): AIBN (16 mg, 0.1 mmol) was added to a solution of 3-(1-cyclohexenylethyl)-2-iodo-3-methyl-1-cyclopentanone (**29**) (664 mg, 2.0 mmol) and tributyltin hydride (582 mg, 2.0 mmol) in dry benzene (400 mL). The solution was stirred for 4.5 h under reflux and then concentrated in vacuo. The residue was purified by column chromatography (cyclohexane/EtOAc, 90:10) and the isomers were separated by HPLC (cyclohexane/EtOAc, 92.5:7.5) to afford **15a** and **15b** (170 mg, 42%). The diastereoisomeric ratio was determined by GC directly from the reaction mixture (**15a:15b**, 52:48).

Acknowledgments

Financial support by the Ministerium für Schule, Wissenschaft und Forschung des Landes Nordrhein-Westfalen (MSWF-NRW), the Deutsche Forschungsgemeinschaft (DFG), the Fonds der Chemischen Industrie, and the Innovationsfonds der Universität Bielefeld is gratefully acknowledged. We also thank the state of Nordrhein-Westfalen for granting a predoctoral scholarship to J. O. B. We wish to thank Prof. Dr. W. W. Schoeller for his support concerning the calculations and Dr. Michael Oelgemöller for his help in preparing the manuscript.

- [1] P. Brownbridge, *Synthesis* **1983**, 1–28.
- [2] P. Brownbridge, *Synthesis* **1983**, 85–104.
- [3] I. Fleming, A. Barbero, D. Walter, *Chem. Rev.* **1997**, *97*, 2063–2192.
- [4] G. M. Rubottom, M. I. Lopez Nieves, *Tetrahedron Lett.* **1972**, *24*, 2423–2425.
- [5] E. Friedrich, W. Lutz, *Chem. Ber.* **1980**, *113*, 1245–1263.
- [6] S. Sakaguchi, Y. Yamamoto, T. Sugimoto, H. Yamamoto, Y. Ishii, *J. Org. Chem.* **1999**, *64*, 5954–5957.
- [7] S. Stankovic, J. H. Espenson, *J. Org. Chem.* **1998**, *63*, 4129–4130.
- [8] K. Kaneda, K. Nobuyoshi, K. Jitsukawa, S. Teranishi, *Tetrahedron Lett.* **1981**, *22*, 2595–2598.
- [9] G. M. Rubottom, J. M. Gruber, R. K. Boeckman Jr., M. Ramaiah, J. B. Medwid, *Tetrahedron Lett.* **1978**, *19*, 4603–4606.
- [10] P. A. Zoretic, M. Wang, Y. Zhang, Z. Shen, A. A. Ribiero, *J. Org. Chem.* **1996**, *61*, 1806–1813.
- [11] Y. Horiguchi, E. Nakamura, E. Kuwajima, *Tetrahedron Lett.* **1989**, *30*, 3323–3326.
- [12] W. Adam, R. T. Fell, C. R. Saha-Möller, C.-G. Zhao, *Tetrahedron: Asymmetry* **1998**, *9*, 397–401.
- [13] J. P. McCormick, W. Tomasik, M. W. Johnson, *Tetrahedron Lett.* **1981**, *22*, 607–610.
- [14] J. O. Bunte, J. Mattay in *CRC Handbook of Organic Photochemistry and Photobiology* (Eds.: W. M. Horspool, F. Lenzi), CRC Press, Boca Raton, 2nd ed., CRC Press, Boca Raton, USA, **2004**, chapters 10, 10.1–10.16.
- [15] D. L. Wright, C. R. Whitehead, E. H. Sessions, I. Ghiviriga, D. A. Frey, *Org. Lett.* **1999**, *1*, 1535–1538.
- [16] K. D. Moeller, M. R. Marzabadi, D. G. New, M. Y. Chiang, S. Keith, *J. Am. Chem. Soc.* **1990**, *112*, 6123–6124.
- [17] C. M. Hudson, M. R. Marzabadi, K. D. Moeller, D. G. New, *J. Am. Chem. Soc.* **1991**, *113*, 7372–7385.
- [18] M. Schmittl, M. Keller, A. Burghart, *J. Chem. Soc., Perkin Trans. 2* **1995**, 2327–2333.
- [19] B. B. Snider, T. Kwon, *J. Org. Chem.* **1992**, *57*, 2399–2410.
- [20] J.-P. Gourvès, R. Ruzziconi, L. Vilarroig, *J. Org. Chem.* **2001**, *66*, 617–619.
- [21] R. Rathore, J. K. Kochi, *J. Org. Chem.* **1996**, *61*, 627–639.
- [22] C. A. Ramsden, R. G. Smith, *Org. Lett.* **1999**, *1*, 1591–1594.
- [23] T. M. Bockman, D. Shukla, J. K. Kochi, *J. Chem. Soc., Perkin Trans. 2* **1996**, 1623–1632.
- [24] T. M. Bockman, J. K. Kochi, *J. Chem. Soc., Perkin Trans. 2* **1996**, 1633–1643.
- [25] A. Heidbreder, J. Mattay, *Tetrahedron Lett.* **1992**, *33*, 1973–1976.
- [26] L. Ackermann, A. Heidbreder, F. Wurche, F.-G. Klärner, J. Mattay, *J. Chem. Soc., Perkin Trans. 2* **1999**, 863–869.
- [27] S. Hintz, R. Fröhlich, J. Mattay, *Tetrahedron Lett.* **1996**, *37*, 7349–7352.
- [28] S. Hintz, J. Mattay, R. van Eldik, W.-F. Fu, *Eur. J. Org. Chem.* **1998**, 1583–1596.
- [29] J. O. Bunte, S. Rinne, J. Mattay, *Synthesis* **2004**, 619–633.
- [30] D. P. Curran, C.-T. Chang, *J. Org. Chem.* **1989**, *54*, 3140–3157.
- [31] J. O. Bunte, S. Rinne, C. Schäfer, B. Neumann, H.-G. Stammer, J. Mattay, *Tetrahedron Lett.* **2003**, *44*, 45–48.
- [32] H. Rinderhagen, J. Mattay, *Chem. Eur. J.* **2004**, *10*, 851–874.
- [33] D. P. Curran, N. A. Porter, B. Giese, *Stereochemistry of Radical Reactions*, VCH, Weinheim, **1996**.
- [34] J. Fossey, D. Lefort, J. Sorba, *Free Radicals in Organic Chemistry*, Wiley, Chichester, New York, **1995**.
- [35] B. B. Snider, B. O. Buckman, *J. Org. Chem.* **1992**, *57*, 4883–4888.
- [36] Y. D. Vankar, G. Kumaravel, *Tetrahedron Lett.* **1984**, *25*, 233–236.
- [37] All calculations were conducted using *TITAN V1.05*, Schrödinger Inc., Wavefunction Inc., **2000**, Schrödinger Development Staff: M. D. Beachy, Y. Cao, R. B. Murphy, J. K. Perry, W. T. Pollard, M. N. Ringnalda, G. R. Yacek, J. R. Wright;

- Wavefunction Development Staff; B. J. Deppmeier, A. J. Driessen, W. J. Hehre, J. A. Johnson, P. E. Klunzinger, M. Wana-tabe, J. Yu.
- [38] H. Fischer, L. Radom, *Angew. Chem.* **2001**, *113*, 1380; *Angew. Chem. Int. Ed.* **2001**, *40*, 1340–1371.
- [39] H. Zuilhof, J. P. Dinnocenzo, A. C. Reddy, S. Shaik, *J. Phys. Chem.* **1996**, *100*, 15774–15784.
- [40] A. D. Becke, *Phys. Rev. A* **1988**, *38*, 3098–3100.
- [41] C. Lee, W. Yang, R. G. Parr, *Phys. Rev. B* **1988**, *37*, 785–789.
- [42] P. C. Hariharan, J. A. Pople, *Chem. Phys. Lett.* **1985**, *82*, 270.
- [43] X. Fang, H. Xia, H. Yu, X. Dong, M. Chen, Q. Wang, F. Tao, C. Li, *J. Org. Chem.* **2002**, *67*, 8481–8488.
- [44] A. L. J. Beckwith, C. J. Easton, A. K. Serelis, *J. Chem. Soc., Chem. Commun.* **1980**, 482–483.
- [45] A. L. J. Beckwith, T. Lawrence, A. K. Serelis, *J. Chem. Soc., Chem. Commun.* **1980**, 484–485.
- [46] D. C. Spellmeyer, K. N. Houk, *J. Org. Chem.* **1987**, *52*, 959–974.
- [47] The complete collection of calculated structures and transition states is available in the supporting information.
- [48] J. Fossey, D. Lefort, J. Sorba, *Free Radicals in Organic Chemistry*, Wiley, Chichester, New York, **1995**, p. 289.
- [49] Landolt-Börnstein, *Numerical Data and Functional Relationships in Science and Technology, Group II: Molecules and Radicals, Volume 13, Subvolume A: Carbon-Centered Radicals I*, Springer, <http://www.landolt-boernstein.com>, p. 289.
- [50] G. K. S. Prakash, C. Bae, G. Rasul, G. A. Olah, *J. Org. Chem.* **2002**, *67*, 1297–1301.
- [51] C. A. Reed, *Acc. Chem. Res.* **1998**, *31*, 325–332.
- [52] P. P. Gaspar, *Science* **2002**, *297*, 785–786.
- [53] J. P. Foster, F. Weingold, *J. Am. Chem. Soc.* **1980**, *102*, 7211–7218.
- [54] A. E. Reed, F. Weinhold, *J. Chem. Phys.* **1983**, *78*, 4066–4073.
- [55] A. E. Reed, R. B. Weinstock, F. Weinhold, *J. Chem. Phys.* **1985**, *83*, 735.
- [56] J. E. Carpenter, F. Weinhold, *J. Mol. Struct. (Theochem)* **1988**, *169*, 41–62.
- [57] Calculations for **50** → **58** were conducted using B3LYP/6–31G*; for **51** to **59**, calculations were conducted using B3LYP/3–21G*.
- [58] N. L. Bauld, *Radicals, Ion Radicals and Triplets, The Spin-Bearing Intermediates of Organic Chemistry*, Wiley-VCH, New York, **1997**, p. 159.
- [59] J. H. Horner, E. Taxil, M. Newcomb, *J. Am. Chem. Soc.* **2002**, *124*, 5402–5410.
- [60] J. P. Dinnocenzo, S. Farid, J. L. Goodman, I. R. Gould, W. P. Todd, S. L. Mattes, *J. Am. Chem. Soc.* **1989**, *111*, 8973–8975.
- [61] O. Poizat, G. Buntinx, P. Valat, V. Wintgens, M. Bridoux, *J. Phys. Chem.* **1993**, *97*, 5905–5910.
- [62] W. L. F. Armarego, D. D. Perrin in *Purification of Laboratory Chemicals*, Butterworth-Heinemann, Oxford, 4th ed., **1996**.
- [63] E. J. Kantorowski, S. W. E. Eisenberg, W. H. Fink, M. J. Kurth, *J. Org. Chem.* **1999**, *64*, 570–580.
- [64] B. B. Kikani, J. T. McKee, M. Zanger, *Synthesis* **1990**, 176.
- [65] E. Campaigne, T. P. Selby, *J. Heterocycl. Chem.* **1980**, *17*, 1255.
- [66] R. Fuchs, J. F. McGarrity, *Synthesis* **1992**, 373.
- [67] L. Duc, J. F. McGarrity, T. Meul, A. Warm, *Synthesis* **1992**, 391.

Received February 24, 2004